Master Thesis

M.Sc. Biological Oceanography

Effects of Warming and Ocean Acidification on Calcification and Photosynthesis of Arctic Coralline Red Algae under Summer Light Conditions

Dana Hellemann

Dipl. Biol. Jan Büdenbender

Prof. Dr. Ulf Riebesell

Prof. Dr. Frank Melzner

April 2012

Christian-Albrechts-Universität zu Kiel

Mathematisch-Naturwissenschaftliche Fakultät

Sektion Meereswissenschaften

GEOMAR Helmholtz-Zentrum für Ozeanforschung Kiel

Abstract

Rising anthropogenic CO_2 emissions since the pre-industrial time are warming the atmosphere and lead to an enhanced uptake of heat and CO_2 into the ocean, resulting in increasing sea surface temperature (ocean warming (OW)), decreasing ocean pH (ocean acidification (OA)) and decreasing carbonate saturation state. Arctic surface waters are projected to become partly undersaturated with respect to aragonite already within this century. Calcified crustose coralline algae (CCA) are regarded sensitive to dissolution due to their high amount of magnesium carbonate, being more soluble than aragonite. Warming might add to CO_2 stress, resulting in potential synergistic effects on calcification in CCA. Knowledge on the calcification process in CCA is limited, however, a linkage to energy generating processes (photosynthesis and respiration) is assumed.

To test for single and synergistic effects of OW and OA on calcification and energy generating processes in Arctic CCA, *Lithothamnion glaciale* was incubated for two months under a cross-factorial design of elevated temperatures (3.5°C, 5.5°C and 7.5°C target values) and elevated pCO_2 (390, 560, 840, 1120 μatm target values) (12 treatment combinations, n = 4 + 1 blank). Light conditions simulated Arctic summer (12 μmol photons m^{-2} s^{-1}). In a side experiment, photosynthetic O_2 evolution (O_2E) and respiratory O_2 consumption (O_2C) were measured optode based under control and treatment conditions.

Mean calcification rates decreased over the experimental duration and with increasing pCO_2, except for the lowest temperature, where calcification was constantly reduced with increasing pCO_2. Dissolution occurred first at the end of the experiment and only in the highest temperature treatment. Relative calcification rates at highest temperature increased at low and intermediate pCO_2 levels and decreased first at a pCO_2 $\succ$1000 μatm. These results indicate a negative synergistic effect for high pCO_2 and elevated temperature, as well as a positive synergistic effect of intermediate pCO_2 and elevated temperature. Results of relative O_2E and O_2C rates indicate a strong linkage between calcification and energy generating processes.

From this study one can conclude, that within this century the Arctic coralline alga *L. glaciale* might not be negatively affected by elevated temperatures and pCO_2 during the Arctic summer season, but rather might profit from those conditions by increasing its calcification rates. Negative effects of elevated temperatures and pCO_2 on *L. glaciale* during the Arctic summer season are first expected for a combination of temperature and pCO_2, that is not predicted to occur within this century for the Arctic Ocean.

Contents

List of Figures

List of Tables

1 Introduction

Increasing carbon dioxide (CO_2) emissions since the industrial age are changing the atmospheric CO_2 concentration and owing to radiative forcing the atmospheric heat content. The Earth's atmosphere is getting warmer and richer in CO_2. The ocean takes up heat and CO_2 from the atmosphere, resulting in increasing sea surface temperatures (Levitus *et al.*, 2005) (ocean warming) and decreasing ocean pH (Caldeira & Wickett, 2003) (ocean acidification) as well as decreasing carbonate saturation state (Orr *et al.*, 2005).

The Arctic Ocean is considered particular sensitive to the impact of global climate change (ACIA, 2005), mainly due to the existence of feedback processes, which might enhance ocean warming, e.g. the albedo-feedback (Loeng *et al.*, 2005), and a naturally low carbonate saturation state (Orr *et al.*, 2005). The Arctic Ocean is assumed to become faster undersaturated with respect to carbonate saturation than other oceans (Orr *et al.*, 2005). Particular calcifying species are likely threatened by carbonate undersaturation (Guinotte & Fabry, 2008).

Calcifying crustose coralline red algae (CCA) are an important part of the Arctic benthic ecosystem (Adey & Macintyre, 1973). CCA are abundant primary producers and significant contributers to coastal calcium carbonate ($CaCO_3$) deposition (Nelson, 2009). The three-dimensional structure of CCA rhodoliths provides microhabitats for diverse species (Foster, 2001) and increases the biodiversity of the habitat (BIOMAERL Team, 2003). CCA deposit $CaCO_3$ in the form of high magnesium calcite (Mg-calcite), which has a higher solubility than aragonite or calcite (Andersson *et al.*, 2008). Under ongoing CO_2 emissions (SRES A2, IPCC 2000), 10% of Arctic surface waters are projected to become undersaturated with respect to aragonite within the coming decades (Steinacher *et al.*, 2009). Based on higher solubility, organisms building up high Mg-calcite, like CCA, are expected to face corrosive conditions even earlier (Andersson *et al.*, 2008). Details on the calcification process in CCA are limited, however, calcification is assumed to be linked to energy generating processes, e.g. photosynthesis or respiration (Borowitzka, 1982; Okazaki, 1977).

So far, the physiological responses of Arctic CCA to the combined effects of ocean acidification (OA) and ocean warming (OW) have not been investigated. Since the future ocean is considered to change in respect to both OW and OA, synergistic effects are likely and might be different to single effects. Therefore, this study aims to answer the following questions: what are the single and synergistic effects of OA and OW on calcification and photosynthesis of the Arctic CCA *Lithothamnion glaciale*? Does OW interact with reported negative OA effects on calcification? Do effects on calcification rates correlate with photosynthesis rates, arguing for a linkage between both processes? Which implications could be drawn from our findings for the Arctic CCA species *L. glaciale* under future ocean conditions?

I tested the Arctic CCA *Lithothamnion glaciale* in 12 different combinations of elevated pCO_2 and temperature levels on their response in calcification and photosynthesis rates. The experiment lasted three months and simulated Arctic summer conditions of polar day (24 h light).

Hypothesis and Assumptions

The experiment was based on the hypothesis that elevated pCO_2 and temperature might show single or synergistic effects on calcification and photosynthesis rates in the Arctic CCA *Lithothamnion glaciale* under summer light conditions. The two main questions are:

a. What are the effects of the applied treatment on calcification and photosynthesis, i.e. how are respective rates affected? Calcification and photosynthesis are assumed to be directly affected by elevated pCO_2 and temperature due to changes in carbonate chemistry and temperature dependent metabolic activity, compare table 1. Synergistic effects of elevated pCO_2 and temperature might change assumed responses.

b. Do both processes responde in accordance with each other, indicating a linkage between calcification and photosynthesis? Assuming that calcification and photosynthesis might be linked by energy, both processes might be indirectly affected by the treatments due to changes in energy availability: if energy storage during photosynthesis (ATP, CO_2-fixation in starch) changes, it could affect consequently energy liberation during respiration, depending on available energy, and calcification, being in need of energy.

Table 1: Assumed impacts of elevated pCO_2 and temperature on calcification and photosynthesis.

	Calcification	Photosynthesis
Elevated pCO_2	Decreasing concentrations of ${CO_3}^{2-}$, could reduce the availability as substrate for calcification (Guinotte & Fabry, 2008).	A lowering pH might impair enzyme activity (Calvin-cycle, cellular respiration) and proton-gradients (light-dependent reaction).
	A decreasing carbonate saturation state could lead to dissolution below $\Omega \prec 1$ to $CaCO_3$ (Fabry *et al.*, 2008).	A higher concentration of dissolved inorganic carbon (DIC) could increase the substrate availability for CO_2-fixation (Riebesell *et al.*, 2007).
Elevated temperature	Changes in carbonate chemistry: decreasing gas solubility according to Henry's law and alteration of temperature-dependent dissociation constants, shifting the relative proportions of inorganic carbon species (Zeebe & Wolf-Gladrow, 2001).	Increasing temperatures generally increase physiological processes (Sommer, 1998), e.g. cellular respiration rates.

Most studies, which investigated the effects of global change (ocean warming and ocean acidification) on CCA, have focused on the response of tropical and temperate CCA to elevated pCO_2 alone, revealing an overall negative CO_2 effect (Kuffner *et al.*, 2008, Jokiel *et al.*, 2008, Hofmann *et al.*, 2011, Büdenbender *et al.*, 2011). So far, only the study of Martin & Gattuso (2009) investigated the effect of elevated pCO_2 in combination with elevated temperature on Mediterranean CCA, revealing synergistic effects of both factors: Net calcification decreased under the combined treatment of high temperature and high CO_2, while pCO_2 and temperature alone showed no effect. Polar CCA are poorly studied so far: Büdenbender *et al.* (2011) is until now the only study dealing with polar CCA. Büdenbender *et al.* (2011) showed, that calcification rates significantly decreased under Arctic summer and winter light conditions. The CO_2 level, at which calcification started to decrease, was different between the seasons: Calcification decreased already at a pCO_2 of 750 μatm in winter and experienced net dissolution, whereas in summer only CCA in the highest pCO_2 treatment (1570 μatm) experienced net dissolution.

A linkage between photosynthesis and calcification has been suggested by Okazaki (1977), Digby (1977) and Borowitzka (1982), who reported light stimulation of calcification, e.g. a 10-fold faster $CaCO_3$ deposition under light than in the dark (Borowitzka, 1982).

1.1 Marine Impacts of Global Climate Change

Global climate change is widely recognized as a consequence of anthropogenic increased emissions of climate relevant greenhouse gases, leading to enhanced radiative heating (Mitchell, 1989). Atmospheric temperatures have already increased stronger than can be explained by natural variability (IPCC, 2001). CO_2 and water vapour are the most important greenhouse gases (Mitchell, 1989). Since the industrial revolution CO_2 emissions are continuously rising (Raupach *et al.*, 2007), leading to increasing atmospheric CO_2 concentrations with a recent concentration of 394 parts per million (ppm) (ESRL/NOAA, March 2012) compared to pre-industrial concentrations of 280 ppm (Canadell *et al.*, 2007). Compared to reconstructed Earth history the recent rate of emitted CO_2 is outstanding among the past 22 000 years (Joos & Spahni, 2008).

The main sources for CO_2 emissions are anthropogenic fossil fuel combustion, industrial processes and changes in land use, i.e. deforestation. In the coming years, growth of the world population and economy, as well as industrial growth of developing countries will most likely further increase CO_2 emissions (Raupach *et al.*, 2007). According to model projections (NCAR CSM 1.4-carbon model) based on the SRES high-emission A2 storyline (IPCC, 2000) future emissions might reach an output

of 30 Gt yr^{-1}, leading to atmospheric CO_2 concentrations of around 840 ppm by the end of this century (Steinacher *et al.*, 2009). A decreasing trend in the capacity of land and ocean sinks for CO_2 uptake has already been observed (Canadell *et al.*, 2007).

With respect to the marine environment, climate change has two impacts: ocean warming as consequence of atmospheric warming and ocean acidification as consequence of a CO_2 equilibration between the atmosphere and the marine system, the so called "*other* CO_2 problem" (Henderson, 2006).

1.1.1 Ocean Warming

Surface ocean and atmospheric heat exchange based on thermodynamic equilibrium is leading to an uptake of atmospheric heat into the ocean (Mitchell, 1989). Significant changes in surface sea temperature (SST) have been recorded since the 1960s (Levitus *et al.*, 2005). In the following 40 years the oceans took up about 84% of total Earth system heat (Levitus *et al.*, 2005). The strongest changes in SST have been observed in the Atlantic with an 75% increase in ocean heat content for the upper 300m in the period 1955 till 2003 (Levitus *et al.*, 2005). Barnett *et al.* (2005) could show that the warming signal was not caused by natural variability, but likely had an anthropogenic origin. According to model projections (NCAR CSM 1.4-carbon model) based on SRES B2 and A2 (IPCC, 2000) global mean SST will further increase by 0.5 - 1.5°C until the end of this century (Steinacher *et al.*, 2009).

Responses of the ocean to increased SST are complex. Overall, ocean warming is predicted to strengthen the stratification of the surface ocean (Bopp *et al.*, 2001, Sarmiento *et al.*, 2004). A strengthening in stratification could reduce the mixing depth of the surface water column, which most likely reduces the supply of new nutrients from deeper water masses. This could change pelagic productivity with consequences for marine food webs and the deep ocean (Bopp *et al.*, 2001, Sarmiento *et al.*, 2004). Furthermore, microbial activity and physiological responses of both pelagic and benthic flora and fauna are likely affected by elevated SST.

1.1.2 Ocean Acidification

The surface ocean and the atmosphere are in a permanent dynamic equilibrium with respect to element concentrations, e.g. $[CO_2]$. In consequence, the oceanic CO_2 concentration rises as atmospheric CO_2 concentration rises. The ocean is considered the biggest sink for atmospheric CO_2 and has already taken up about one third of total anthropogenic CO_2 emissions (Sabine *et al.*, 2004). CO_2 that enters the ocean changes the ocean's carbonate system by forming carbonic acid (H_2CO_3), which dissociates into bicarbonate HCO_3^- and carbonate CO_3^{-2} ions as well as free protons $[H^+]$ (eq. 1).

$$CO_2 + H_2O \rightleftharpoons H_2CO_3 \rightleftharpoons HCO_3^- + H^+ \rightleftharpoons CO_3^{-2} + 2H^+ \quad (1)$$

A part of H^+ is buffered by $CO_3{}^{-2}$ ions (Kleypas & Langdon, 2006), which reduces the ocean's buffer capacity and loweres the carbonate saturation state (Orr *et al.*, 2005, Kleypas & Langdon, 2006, Fabry *et al.*, 2008). Additionally, the carbonate system is shifted to higher $HCO_3{}^-$ concentrations (Sabine *et al.*, 2004). According to model projections (Steinacher *et al.*, 2008) based on the SRES A2 storyline (IPCC, 2000) the total ocean fraction of oversaturated water might decrease by 17% over this century. Remaining free H^+ increase in total H^+ concentration (Orr *et al.*, 2005), which is measurable in the lowering ocean pH; the ocean becomes more acidic, it "acidifies" (Caldeira & Wickett, 2003). Ocean surface pH has already dropped by 0.1 units since pre-industrial times (Caldeira & Wickett, 2003), which translates to an increase in H^+ concentration by 30% (Fabry *et al.*, 2008). The mean surface ocean pH is expected to further decrease by 0.3 - 0.4 units until the end of this century (Caldeira & Wickett, 2003). Assuming unabated CO_2 emissions, ocean pH might even drop by 0.7 units until the year 2300, which would be a lower pH than the ocean has ever experienced in the past 300 million years (Caldeira & Wickett, 2003).

Especially calcifying organisms are expected to suffer from changes in carbonate chemistry (Riebesell *et al.*, 2000, Orr *et al.*, 2005, Fabry *et al.*, 2008): their shells and skeletons made of calcite, aragonite or magnesium-calcite are likely to dissolve in undersaturated water (eq. 2), while the ability to increase calcification rates (eq. 3) could be negatively affected by reduced substrate availability (Guinotte & Fabry, 2008).

$$CaCO_3 + CO_2 + H_2O \rightarrow Ca^{2+} + 2HCO_3^- \tag{2}$$

$$Ca^{2+} + 2HCO_3^- \rightarrow CaCO_3 + CO_2 + H_2O \quad respect. \quad Ca^{+2} + HCO_3^- \rightarrow CaCO_3 + H^+ \tag{3}$$

Geological records revealed that ocean acidification events have happened before in Earth's history. The major difference between past and recent acidification is the rate of change: while past events occurred slowly over millions of years, e.g. climate change due to plate tectonics (Caldeira & Wickett, 2003), the actual rate of CO_2 uptake into the ocean is much faster (Joos & Spahni, 2008).

1.1.3 The Changing Arctic

The Arctic is considered particular sensitive to the impact of global climate change (ACIA, 2005). In terms of climate warming, the Arctic is assumed to warm faster than the global average (polar amplification) due to cumulative effects of feedback processes (e.g. albedo-, thermohaline- and greenhouse gas-feedback (Loeng *et al.*, 2005)) and a climate, which is strongly associated to sea ice-

atmosphere processes (McBean *et al.*, 2005). Over the past 100 years the mean air temperature has already increased by 0.09°C per decade (based on data form the Global Historical Climatology Network) (McBean *et al.*, 2005), resulting in a thinning and loss of sea ice and melting of glaciers (ACIA, 2005).

In terms of ocean acidification, Arctic surface waters are projected to become faster undersaturated with respect to carbonate saturation than the global ocean due to a naturally low carbonate saturation state and the low water temperature (Orr *et al.*, 2005). Low water temperatures promote gas solubility according to Henry's law, leading to an enhanced uptake of CO_2 into the Arctic Ocean and a subsequently decreasing pH and carbonate saturation state.

Warming and acidification of surface waters are tightly linked: melting sea ice increases the ocean surface area, which is in direct contact with the atmosphere and consequently takes up CO_2 (Loeng *et al.*, 2005). Freshwater input due to ice melting lowers alkalinity (Steinacher *et al.*, 2009), contributing to low carbonate concentration and buffer capacity. According to model projections based on SRES A2 (IPCC, 2000) warming might increase the uptake of CO_2 by 40%, leading to a 20% higher decrease in saturation state and pH (Steinacher *et al.*, 2009).

In general, the future Arctic Ocean is assumed to become warmer, fresher, stronger stratified and more acidic. In specific, Arctic surface waters are projected to experience a drop in pH by 0.4 units and aragonite undersaturation of nearly the entire water column by the end of this century, when emissions follow SRES A2 (IPCC, 2000) (Steinacher *et al.*, 2008). Already within the coming decades, 10% of the surface water might become undersaturated for at least one month per year (at 409 μatm) or throughout the year (at 450 μatm), establishing corrosive conditions for calcifying organisms made of aragonite or Mg-calcite (Steinacher *et al.*, 2009).

The Arctic Ocean is a marine habitat of extreme conditions, including low water temperatures, partly sea-ice cover, freshwater input, low underwater irradiance and a strong seasonality with respect to light conditions, notably polar day (24 h light) and polar night (24 h darkness) (Freiwald & Henrich, 1994, Loeng *et al.*, 2005). Underwater irradiance is seasonally affected by melt water input, sediment load and stratification in summer as well as sea-ice and snow cover in winter and spring. Reduced transmittance limits the euphotic depth (Svendsen *et al.*, 2002). Productivity follows the prevailing light regime: productivity exhibits a seasonal peak, but is averaged over the year quite low (Loeng *et al.*, 2005). Resident Arctic species are perfectly adapted to these conditions (Loeng *et al.*, 2005), what makes them and their ecosystem particularly sensitive and vulnerable to changes. The adaptation of Arctic species to their extreme habitat likely limits ability to respond to changes (Usher, 2005).

1.2 The Carbonate System of the Ocean

The carbonate system of the ocean is one of the most important chemical equilibria in the ocean. It is responsible for controlling the ocean's pH (Fabry *et al.*, 2008). In the following, the main aspects of the carbonate system will be given according to Zeebe & Wolf-Gladrow (2001). For further reading and more details see for example Zeebe & Wolf-Gladrow (2001).

Surface ocean and atmosphere exchange CO_2 based on thermodynamic equilibrium. CO_2 that enters the ocean reacts with water and forms true carbonic acid (H_2CO_3), bicarbonate (HCO_3^-) and carbonate (CO_3^{2-}) ions as well as protons (H^+) (1.1.2, eq. 1). A small amount of the gaseous CO_2 that is taken up dissolves to aqueous $CO_{2(aq)}$. H_2CO_3 and $CO_{2(aq)}$ are generally treated together, e.g. as CO_2. The equilibrium of the carbonate system and therefore the quantities of the ions is controlled by equilibrium constants (K_1 and K_2)(eq. 4).

$$CO_2 + H_2O \overset{K_1}{\leftrightarrow} HCO_3^- + H^+ \overset{K_2}{\leftrightarrow} CO_3^{2-} + H^+ \tag{4}$$

The carbonate system in seawater can be described with stoichiometric equilibrium constants ($K_1{}^*$, $K_2{}^*$), which are related to concentrations and dependent on temperature, salinity and pressure.

The total dissolved inorganic carbon (DIC) of the ocean is the sum of all dissolved inorganic carbon species (eq. 5).

$$DIC \;=\; [CO_2] + [HCO_3^-] + [CO_3^{2-}] \tag{5}$$

The total alkalinity (TA) (eq. 6) is the "capazity of water to neutralize hydrogen ions" (Smith & Key, 1975). Dickson (1981) gives the following definition: "Total alkalinity of a seawater sample is defined as the number of hydrogen ions equivalent to the excess of proton acceptors (bases formed from weak acids with a dissociation constant $K \leq 10^{-4.5}$ at 25°C and zero ionic strength) over proton donators (acids with $K \succ 10^{-4.5}$) in 1 kg of sample".

$$TA \;=\; [HCO_3^-] \;+\; 2[CO_3^{2-}] \;+\; [B(OH)_4^-] \;+\; [OH^-] \;-\; [H^+] + \textit{minor components} \tag{6}$$

With $K_1{}^*$ and $K_2{}^*$, DIC (eq. 5) and a simplification of (eq. 6) the carbonate system can be described quantitatively. These four equations describe 6 unknown variables: $[CO_2]$, $[HCO_3^-]$, $[CO_3^{2-}]$, $[H^+]$, DIC and TA. In consequence, the carbonate system can be calculated from any known two of these six variables. Yet, it has to be kept in mind, that only $[CO_2]$, $[H^+]$, DIC and TA can be measured directly.

The carbonate saturation state (Ω) is important for the formation and dissolution of calcium carbonate ($CaCO_3$) in the ocean. Ω is a function of [$CO_3{}^{2-}$] (eq. 7, with $K_{sp}{}^*$ being the stoichiometric solubility product for $CaCO_3$). Based on eq. 7, Ω is reduced by the reduction of $CO_3{}^{2-}$ ions with H^+, which mainly originate from CO_2 uptake in water (eq. 1).

$$\Omega = \frac{[Ca^{2+}][CO_3^{2-}]}{K_{sp}^*} \tag{7}$$

At $\Omega \succ 1$, a solution is supersaturated with respect to $CaCO_3$, favouring biogenic $CaCO_3$ precipitation. At $\Omega \prec 1$, a solution is undersaturated with respect to $CaCO_3$, favouring biogenic $CaCO_3$ dissolution.

1.3 Crustose Coralline Red Algae

Crustose coralline algae (CCA) are calcified benthic macroalgae of the phylum Rhodophyta. They are the most calcified algae in the ocean (Littler, 1976), being a major component of the benthic calcium carbonate production (Nelson, 2009). Their rigid appearance and characteristic purple pink colour make them easy recognizable among other benthic algae (compare fig. 2). Yet, they are regarded as a taxonomically difficult to identifying algae group which might explain their underrepresentation in scientific literature (Adey & Macintyre, 1973). Detailed knowledge on ecological aspects and metabolic functions, e.g. their calcification process, is still rare. Recently, CCA got more attention as biological research object in the light of ocean acidification studies due to their strong calcified tissue.
Due to the good conservation of the calcified tissue, CCA comprise a hugh fossil record (Steneck, 1986). Fossil CCA are used in paleosciences in reconstructions of paleoclimate (Foster, 2001) or paleooceanic conditions, e.g. past oceanic Mg/Ca ratios (Ries, 2009). CCA are commercially used as agent for water filtration and as soil conditioner (Foster, 2001). However, due to their slow growth, CCA are considered a non-renewable resource (BIOMAERL Team, 2003).

Taxonomic Classification (Guiry & Guiry, 2012)

In the phylum of Rhodophyta CCA belong to the order of Corallinales, which consists of two families: the Hapalidiaceae and the Corallinaceae. The Hapalidiaceae separate into three subfamilies of which Melobesioideae is the biggest with 180 species. All species are non-articulate, i.e. completely calcified. The Corallinaceae separate into eight subfamilies, of which five consists of non-articulate and three (Amphiroideae, Corallinoideae, Metagoniolithoideae) of articulate, i.e. not completely calcified, species (compare fig.1).

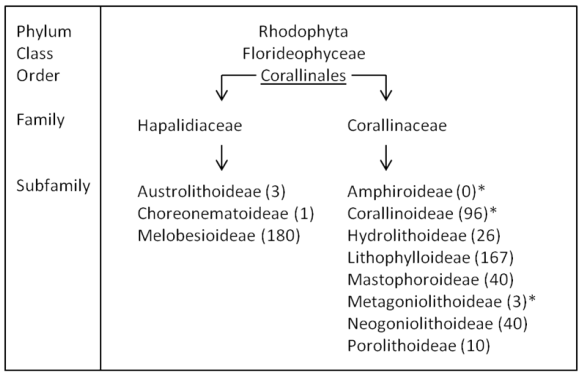

Figure 1: Systematic of the Corallinales accoring to Guiry & Guiry (2012). Numbers in brackets are species numbers, asterics indicate articulate species.

Figure 2: Crustose Coralline red algae *Lithothamnion glaciale* from the Kongsfjord, Svalbard, Norway. Specimens belong to the experimentally used algae.

Distribution and Habitat

CCA are worldwide abundant (Adey & Macintyre, 1973). They occur over a broad range of temperature regimes in the benthic photic zone of all oceans from Arctic to Antarctic (reviewed by Steneck, 1986). Their depths distribution ranges within the photic zone from the shallow intertidal to the lower end of the photic zone (Adey & Macintyre, 1973). CCA have a low light requirement and can live at great depths (Foster, 2001) close to light compensation conditions (Schwarz *et al.*, 2005). CCA primarily occur on hard substrata in areas with sufficient water energy (Adey & Macintyre, 1973). Free-living forms can also be found on sediment bottoms with less water energy where they accumulate to large communities (Foster, 2001). In tropical waters CCA are tightly associated with coral reefs (reviewed by Littler, 1972).

Morphology and Growth Forms

CCA morphology and growth forms are divers and influenced by prevailing habitat conditions, e.g. water turbulence and depth (reviewed by Steneck, 1986). The three main growths forms are: crusts (completely attached to a substrate), "leafy"-forms (partly attached with unattached margins) and free-living forms (completely unattached) (Steneck, 1986). According to their degree of calcification, CCA divide into articulate and non-articulate species. Articulate species have uncalcified joints, which make them more flexible (Johansen, 1981). From presently known 605 coralline species 99 are articulate (Guiry & Guiry, 2012). Non-articulate species are completely calcified (Johansen, 1981). They grow attached as thin or thick crusts or free living as maerl and rhodoliths (Steneck, 1986). Maerl originates from fragments of crust protuberances. Those fragments continue to grow freely by protuberance elongation, which leads to a delicate, branched shape (Johansen, 1981). Rhodoliths originate from spore settlement on an unstable organic or inorganic substrate, e.g. mussels, stones (Adey &

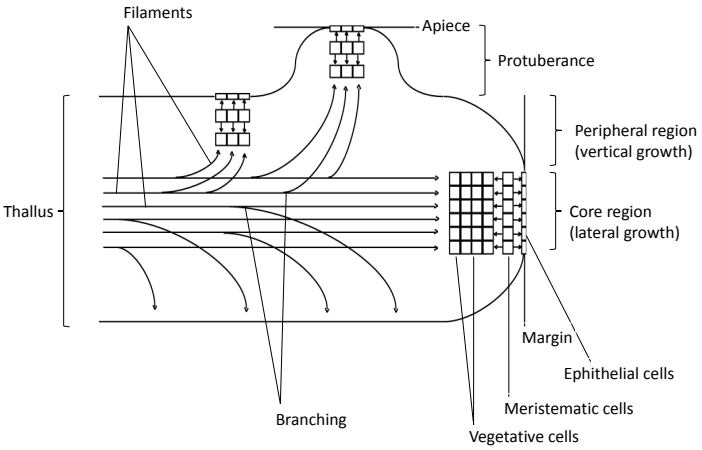

Figure 3: Schematic section through a branch showing filament organisation in CCA. Boxes symbolize meristematic regions where growth takes place, arrows indicate the direction of growth.
Graphic provided by J. Büdenbender.

Macintyre, 1973). They grow as crust layers around those nuclei, which are either permanent incorporated into the rhodolith or decomposed with time (Johansen, 1981), leaving a characteristic hollow core. Rhodoliths have a three-dimensional, roughly spherical shape with abundant protuberances (Johansen, 1981).

In spite of their free-living lifestyle rhodoliths can accumulate to large communities, so called "rhodolith beds" (Foster, 2001). According their area cover, Foster (2001) ranks rhodolith beds with kelp beds and forests, seagrass meadows and non-articulated coralline reefs. He suggests rhodolith beds to be one of the four major benthic macroalgae communities in the ocean.

1.3.1 Cellular Anatomy and Function (according to Johansen, 1981)

Tissue of CCA is arranged in filaments. Filaments build a thallus that consists of an inner (hypo-) and an outer (perithallus) part. In crusts, hypothallial tissue is build by the lowermost filaments, which are oriented parallel to the substrate. Perithallial tissue is build by the uppermost filaments of the hypothallus. Filaments of the perithallial tissue arch perpendicular away from the hypothallus towards the crust surface and end in small epithallial cells, building a cell layer (epithallium) comparable to an epidermis. In rhodoliths, filaments are similar orientated with the exception, that hypothallial tissue is organized in a central "core" (Woelkerling, 1988), being surrounded by perithallial tissue. Consequently, perithallial filaments arch to all sides (compare fig. 3).

Tissues can be distinguished by the cell length with epithallus cells $\prec$ perithallus cells $\prec$ hypothallus cells. Cells of a filament are joined vertically by primary pit-connections, which originate during cell division, being closed by a pit plug. Cells can also be joined laterally by secondary pit-connections and cell fusions. Secondary pit-connections are narrow channels through the cell wall of adjacent cells, closed by a pit plug. Cell fusions link adjacent cells without any plug. They originate as the cell wall

between two cells dissolves and the nuclei of both cells fuse to form a new cell. Both lateral and vertical connections are assumed to be important for the transport of photosynthates from photosynthetic active to unactive (Steneck, 1986) or shaded (Dethier & Steneck, 2001) tissue cells. Algae grow by cell division of meristematic cells in the upper perithallial tissue. Meristematic cells lay either below epithallial cells (intercalary meristem) or at the top end of perithallial cells when epithallial cells are absent (primary meristem). Primary meristems are mostly found where intense growth occurs, e.g. branch tips. Dividing meristematic cells produce both perithallial and epithallial tissue (Steneck, 1986). Dead epithallial cells are discharged in a "sloughing" process (Johansen, 1981) and replaced by new cells. Sloughing is discussed as a way to keep the epithallial surface clean of epiphytes (Borowitzka & Vesk, 1978). Meristematic cells also produce reproductive cells by cell differentiation. Reproductive cells are contained in roofed chambers (conceptacles) at the surface of crusts or protuberances, opening by a single or multiple pores to the surrounding water. Photosynthesis takes place in epi- and upper perithallial tissue, which is indicated by a high number of chloroplasts. Starch grains are stored depper in the tissue (Borowitzka & Vesk, 1978). Nutrients are taken up by epithallial cells (Johansen, 1981).

1.3.2 Ecology

Low-Light Adaptation

CCA grow best under low light intensities (Johansen, 1981), which enables them to occupy habitats in great depths up to 200 m or in the shade of other plants (compare Adey & Macintyre, 1973). This low light adaptation might be based on a more efficient absorption of low light and /or a high ability to fix and store CO_2 during photosynthesis (Steneck, 1986, Schwarz *et al.*, 2005). Schwarz *et al.* (2005) suggest that low-light adaptation might be an explanation for the occurance of CCA in high latitude waters, where irradiance is low and further reduced by ice-cover and strong seasonality regarding polar day and night.

Growth Pattern and Growth Rates

Basic requirements for CCA growth are water motion and low light intensities (Johansen, 1981). Water motion facilitates nutrient supply to the algae and helps mechanical to keep the algal surface clean of epibionts (biofouling)(Steneck, 1986) by rolling rhodoliths against each other. Additionally, biofouling is reduced by grazing of for example snails on CCA surfaces (reviewed by Littler, 1972) and sloughing of epithallial cells (Borowitzka & Vesk, 1978). A clean, unshaded algal surface is important to avoid reductions in photosynthetic productivity (Steneck, 1986). CCA grow via vertical extension, increase in thickness and / or branch elongation (Johansen, 1981). Growth rates are low compared

to uncalcified algae and differ with season, depth and geographical region, i.e. temperature regime (compare an overview given by Foster, 2001). Experimentally estimated growth rates vary between 0.1 - 1.0 mm y^{-1} for temperate maerl (Bosense & Wilson, 2003), 0.4 mm y^{-1} for free-living individuals at depths $\prec$ 20m (Foster, 2001) and $\prec$ 1.0 cm y^{-1} for intertidal crust margins (Dethier & Steneck, 2001).

1.3.3 Calcification

CCA deposit calcium carbonate ($CaCO_3$) in the form of high Mg-calcite (Mackenzie *et al.*, 1983) with an average magnesium carbonate ($MgCO_3$) fraction of 11 - 21 Mol %, occasionally up to 36 Mol %, which is the highest $MgCO_3$ content so far described in any calcifying species (Vinogradov, 1953). High Mg-calcite has a higher solubility than aragonite or calcite (Andersson *et al.*, 2008), which are the most dominant $CaCO_3$ forms in calcifying organisms (Littler, 1976). In CCA, calcite deposition takes place within the cell wall (Borowitzka, 1977). Calcification in CCA is assumed to provide mechanical support and protection against grazing and fouling (Littler, 1976). However, the mechanisms of calcification in CCA are still unknown and detailed knowledge is limited, so far. In the following, the main theories about the calcification process in CCA are described.

The "Organic Matrix Theory" (Borowitzka, 1977) suggests that a protein-polysaccharide complex favours the deposition of calcite due to specific substances contained in these complexes (Borowitzka, 1977). This theory is supported by Lind (1970) who proposed initial crystal nucleation to happen within an electron dense cell wall layer close to the membrane.

The "Bicarbonate Usage Theory" (Borowitzka, 1977) suggests a close relationship between photosynthesis and calcification: HCO_3^-, taken up for photosynthesis, is assumed to be converted by photosynthetically produced OH^- and e^- to CO_3^{2-}, which might subsequently react with Ca^{2+} to $CaCO_3$ (Borowitzka, 1977). The bicarbonate usage theory is not proven so far.

McConnaughey& Whelan (1997) proposed calcification to be a tool for H^+ generation, which supports photosynthetic carbon and nutrient uptake, suggesting that $CaCO_3$ production is only a by-product: Calcification produces H^+ (eq. 3), which could promote the conversion from HCO_3^- to CO_2 for photosynthatic uptake.

Furthermore, McConnaughey& Whelan (1997) proposed that pH-regulation mechanisms could be involved in the calcification process in CCA: elevating the pH at the site of calcification would convert bicarbonate HCO_3^- to carbonate CO_3^{2-} and facilitate calcification. pH-regulation mechanisms are supposed to be energy dependent due active transport of H^+ (McConnaughey& Whelan, 1997).

2 Material and Methods

2.1 Material Collection

Crustose coralline algae used in the experiment originated from Kongsfjorden (79°N, 12°E), an Arctic fjord at the west coast of Svalbard, Norway. An extensive review on the physical environment and marine ecosystem of Kongsfjorden is given by Svendsen *et al.* (2005) and Hop *et al.* (2002). In the fjord, coralline algae are reported to be abundant on subtidal hard-bottom, being an important part of the benthic primary producers (Hop *et al.*, 2005).

Algal material was collected in June 2010 via scuba diving from 8 - 12 m depth at Kongsfjordneset (78°58' N 9°30'E) (fig. 4).

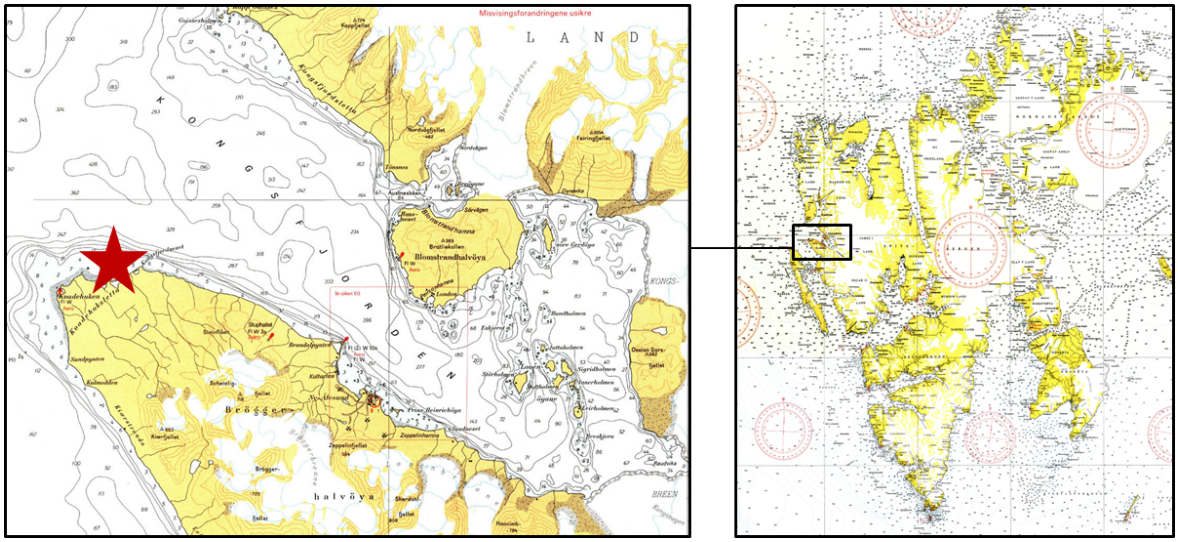

Figure 4: Overview map of Svalbard (right) and detail map of Kongsfjorden (left); the red star marks the sampling location at Kongsfjordneset.

2.1.1 Cultivation and Acclimation in the Lab (GEOMAR)

Algal material was transported from Svalbard to Kiel in 100 l natural fjord water at 3°C. From summer 2010 until spring 2011 algae were kept cultivated in a climate chamber at GEOMAR. Cultivation was done in 2 l natural North Sea water, which was changed every two weeks in order to renew nutrients and total alkalinity. A streaming pump (Hydor, Koralina nano, 1600 l h^{-1}) accounted for a continuous water current in the cultivation water. In order to simulate Arctic winter and summer conditions, algae were kept at no light and 1°C from summer 2010 until spring 2011, and at 6 μmol photons $m^{-}2$ s^{-1} and 4°C from spring 2011 until summer 2011, respectively. Light and temperature between winter and summer season were gradually changed.

2.1.2 Identification

Identification of collected coralline algae (rhodoliths) separated into genus and species identification. For the genus identification rhodolith-forming genera of coralline algae (Harvey & Woelkerling, 2007) were compared with genera lists of the sampling location Spitzbergen (Hansen & Jenneborg, 1996; Vinogradova, 1995 and Athanasiadis, 2006 in Guiry & Guiry, 2012), resulting in four rhodolith-forming coralline genera being described for Spitzbergen: *Phymatolithon, Mesophyllum, Lithothamnion* and *Lithophyllum*. Subsequently, diagnostic key features of the selected genera (Harvey & Woelkerling, 2007) were compared to scanning electron microscopy (SEM) pictures of algae specimens. For SEM pictures three randomly chosen algae individuals were bleached in 10% sodium hypochlorite (NaClO) solution and sectioned according to Woelkerling (1988). SEM pictures were taken with CamScan 44/EDX (Institute for Geosciences, Geologie/Paleontology, Christian-Albrechts University Kiel) and Phenom G2 (FEI Company, GEOMAR, Marine Ecology).

For the species identification the mean cell diameter of 17 surface cells of algal specimens was compared to according measurements from Adey *et al.* (2005). The mean cell diameter was calculated from the longest and shortest distance of surface cells (through the pit-plug until the middel lamella). Since identification of coralline algae is known to be complicated (e.g. Adey & Macintyre, 1973) results of our identification will be genetically validated (Museum National d'Histoire Naturelle, Paris).

2.1.3 Photo Database

Each alga specimen used in the experiment was documentated from front- and backside by means of digital photographs. All pictures were collected in a catalogue, allowing an easy identification of algae specimens, e.g. during buoyant weight measurements or water change. The procedure was repeated after the experiment for reasons of visual comparison.

2.2 Experimental Design

The experimental design included two treatment factors (CO_2 and temperature) at four, repectively three factor levels (target levels 390, 560, 840, 1120 μatm pCO_2 and 3.5, 5.5, 7.5°C) which were cross factorial combined, resulting in 12 distinct treatment combinations.

Each treatment combination was replicated four times with identical incubation units (reactors), containing one alga specimen. Additionally, one reactor per treatment combination contained no alga specimen and served as blank in order to monitor processes in the incubation water, like bacterial activity. The total experimental duration of three months consisted of one month "baseline" and two months treatment and divided into 6 incubation phases of 14 days each, after which sampling took

place and water was renewed. We chose 14 days as duration for the incubation phases as well as a water volume of 2 l for incubation in order to get a significant change in total alkalinity (TA) due to algal calcification.

Baseline

A "baseline" represents in general a response to control condition (Baker & Dunbar, 2000), e.g. the response of an organism to habitat specific in-situ conditions. By comparing an organisms standardized response with its respond to changed conditions, e.g. due to an applied treatment, the effect of the treatment on the organism can be evaluated as percental deviation from the standardized response (eq. 8) (compare Büdenbender *et al.*, 2011).

$$X_{rel}\ (\%)\ =\ \frac{X_{net\ (treatment)}}{X_{net\ (baseline)}} * 100 \tag{8}$$

with X_{rel} = relative change from the baseline (%), $X_{net\ (treatment)}$ = measured net response under treatment conditions and $X_{net\ (baseline)}$ = measured net response under baseline conditions. Responses under baseline conditions are represented by 100%. Relative responses $\succ$ 100% represent higher and relative responses $\prec$ 100% represent lower response rates compared to the baseline.

In our experiment, we run a baseline of one month (two incubation phases) prior to the treatment phase of elevated CO_2 and temperature. During the baseline, all replicates were incubated at ambient conditions of 390 μatm and 3.5°C target levels in order to simulate in-situ Arctic summer conditions. At the end of an incubation phase sampling took place as outlined in 2.4. As coralline algae often contain solid material, like stones (compare 1.3), individual alga specimens used in the experiment could not be standardized to their total weight. Therefore, a baseline was particular important in order to standardize the experimentally used coralline algae.

Treatment

A treatment represents conditions, which are changed compared to ambient, in-situ conditions. In our experiment we implemented the two treatment factors CO_2 and temperature. CO_2 target levels corresponded to present day (ESRL-NOAA data, Mauna Loa Observatory) and two-, three- and four-times pre-industrial CO_2 (Riebesell *et al.*, 2010). CO_2 partial pressure (pCO_2) was elevated in the incubation water by a constant aeration of the water with premixed air enriched with pCO_2 target levels (Riebesell *et al.*, 2010).

Water temperature target levels corresponded to mean in-situ summer temperatures at habitat depth of collected alga material (F. Cottier, personal communication; mooring site at the outer Kongsfjord

from 2003-05, 2007-11) and a model projected increase in surface sea temperature by 2°C from pre-industrial time to the end of this century, according to the SRES A2 scenario (Steinacher *et al.*, 2009). A temperature elevation by 4°C was meant as physiological test for experimentally used algae.

Light Regime

Light-conditions simulated Arctic summer, i.e. polar day with continuous light. Underwater irradiance was calculated for respective habitat depth of collected alga material (12 m) with eq. 9 (D. Hanelt, personal communication):

$$PAR\ (depth) = \ max\ PAR * exp\ (-K_d * depth) \tag{9}$$

with PAR = photosynthetic active radiation (400 - 700 nm) and K_d = vertical attenuation coefficient of downward irradiance. For a depth of 12 m we used a max PAR of 78 W m^{-2} and a K_d of 0.28 m^{-1} (compare Hanelt *et al.* (2001) p. 652 fig. 2 (PAR) and p. 653 fig. 5 (K_d)). For the K_d value we assumed no melt water input due to the sampling location at the outward fjord. Calculated underwater irradiance was 12 μmol photons m^{-2} s^{-1}.

Experimental Terms

Following terms will be used when referring to the experimental design:

- Experimental duration: the total time of the experiment (12 weeks).
- Incubation phase: a period of two weeks under experimental conditions, after which sampling took place and incubation water was renewed; applies to both treatment and baseline phases.
- Treatment phase: a period of two weeks under treatment conditions, after which sampling took place and incubation water was renewed.
- Baseline phase: a period of two weeks under baseline conditions, after which sampling took place and incubation water was renewed.

2.3 Experimental Set-Up

The experimental set-up consisted of three freezer cabinets (in the following: freezers), which were assigned to each one target temperature level. Each freezer held 20 identical incubation units (reactors), which were assigned to four pCO_2 levels (fig 5). Reactors were made of acryl glass with a volume of ~2.5 l each. The 20 reactors were placed in a water bath in order to stabilize temperature fluctuations due to cooling and non-cooling intervalls of the freezers. Freezer temperatures were controlled

with independent temperature control units, which measured the temperature inside the freezer and adjusted it to applied target temperatures. The temperature of the water bath was logged (PreSens, F1Box) and verified with an analogue mercury thermometer. Water bath temperatures were regarded representative for temperatures within the reactors. An implemented streaming pump (Hydor, Koralina nano, 1600 l h^{-1}) maintained a constant water current within each bath.

Reactors were filled with two litres of North Sea water (compare 2.4) and continuously aerated with premixed CO_2 enriched air, which was provided by a gas mixing pump (Vögtlin, Q-flow). Gas with ambient CO_2 originated from compressed air outside of the GEOMAR. Gas was 100% saturated with water vapour by bubbling it through ultrapure water in gas washing bottles (Schott Duran) in order to reduce evaporation in the reactors.

Reactors were of cylindrical shape (radius = 5 cm, height = 40 cm) and made of acryl glass (fig 6). During incubation, reactors were closed by a lid, which contained two holes, closed by rubber plugs: the small hole served for sampling purposes, the bigger hole served for gas supply and outlet by means of two inlets through the rubber plug. Inside the reactor, the gas supply pipe ended in a graphite air stone (aquaria supply), which dispersed the gas. A water current was established by directing the gas bubbles through a vertical acryl glass tube: gas bubbles were released through holes in the upper part of the tube and thereby water was sucked into the tube from its lower end (air lift system) (fig. 6).

Target underwater irradiance of 12 μmol photons m^{-2} s^{-1} was obtained by installing blue fluorescent lamps (Arcadia, Marine Blue 420 nm Actinic T5) at the inner freezer cover and darkening them with grey foil to the desired irradiance. Underwater irradiance was measured before and after the experiment with a light meter (Licor, Li-250A).

Alga specimens were placed on the reactor bottom. Reactors within a water bath were randomly placed and positions were randomly changed after each sampling. This should ensure homogeneous conditions for all reactors as prevailing temperature and light regime showed small variations within the freezers.

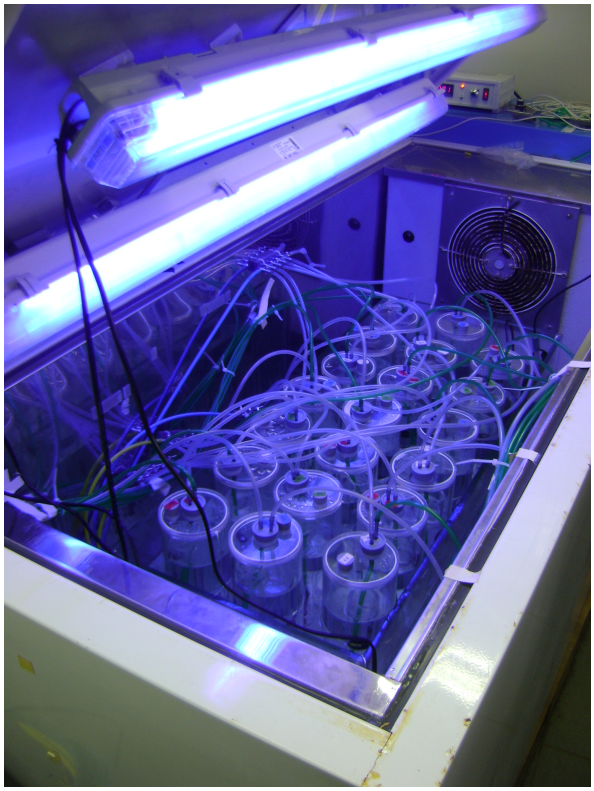

Figure 5: Experimental set-up for the CO_2 and temperature treatment: one of three freezer cabinets, which were assigned to each one target temperature level. The freezer held a water bath with 20 reactors, which were assigned to four pCO_2 levels. CO_2 gas was supplied via pipes from gas mixing pumps. Light from the top simulated Arctic summer light conditions for respective habitat depth of collected alga material (12 μmol m^{-2} s^{-1} for 24 h).

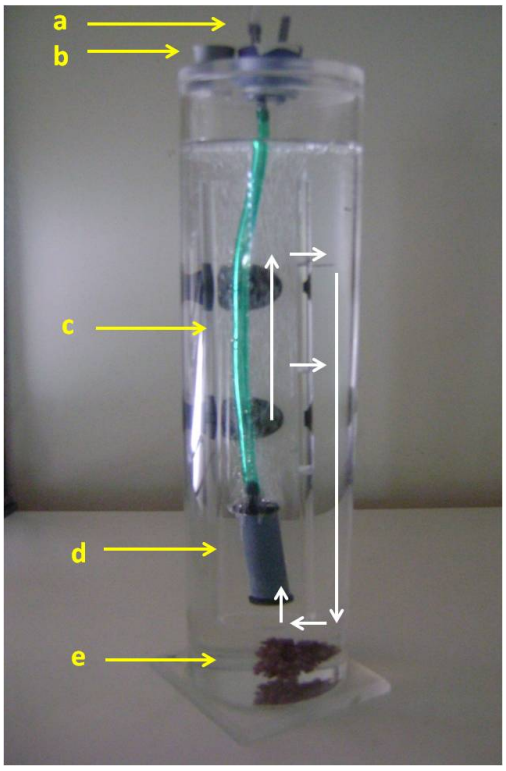

Figure 6: Set-up of an incubation unit (reactor), containing ~2.5 l North Sea water and one alga specimen (e). Incubation water was aerated with CO_2 enriched air via an inlet (a) through a rubber plug in the lid. Another plug (b) closed a hole serving for sampling purposes. Gas was dispersed within the reactors by an graphite air stone (d). A water current (indicated by blue arrows) was established by directing air bubbles through a vertical acryl glass tube with holes (c) (air lift system).

2.4 Experimental Procedure

Experimental procedures included the preparation of incubation water, sampling and change of incubation water to start a new incubation phase. Incubation was done in natural North Sea water with a salinity of 30.4 ± 0.1 before the experiment. Total alkalinity (TA) was increased with sodium carbonate (Na_2CO_3) to around 2366.5 ± 23.6 μmol kg^{-1} according to Key *et al.*, 2004. Nutrient concentrations of the start water were similar to in-situ concentrations measured in the Kongsfjord in June 2010 (EPOCA mesocosm campaign, unpublished data).

North Sea water was kept in 1000 l tanks from which small volumina were regularly taken for the preparation of start water. Start water refers to the water that was used to start a new incubation phase. In order to ensure a mixed water body within the tank before taking water, tank water was

mixed for one day by using a pump (Eheim Universal). Start water was filtered through 0.2 μm glass fiber filters (GF/B, Whatmann) and distributed to four 20 l polycarbonate bottles (Nalgene). For one day all bottles were cooled to $\sim$ 7°C in a climate control room and pre-aerated with CO_2 enriched air to the respective target pCO_2 level. Target pH levels of prepared start water were controlled via a portable pH meter (Metrohm, 826pH). Start water for the first treatment phase was not acidified in order to avoid a "CO_2-shock" for the algae. Instead, water was more slowly acidified in the reactors themselves. For the subsequent treatment phases water was pre-acidified.

The routine for sampling procedures and start of a new phase were as follows: at the beginning of the experiment the empty weight of all reactors was determined with a high precision scale (Sartorius, SR3 2001, precision $\pm$ 0.1 g). After filling with approximately 2 l of start water the full weight was determined in order to calculate the exact incubation volume of each reactor. Each reactor received one alga specimen and incubation was started by connecting reactors to the gas supply. Samples for nutrient and TA analysis were taken from the start water and represented start conditions for all reactors.

After 14 days, incubation was stopped and reactors were weighted again in order to determine potential loss of water. pH, temperature and salinity were recorded (Metrohm, WTW TetraCon 325 with WTW Multi 350i device). Water samples for nutrient and TA analysis were taken with a syringe. Nutrient samples were stored at -20°C. TA samples were poisoned with 20 μl mercuric chloride ($HgCl_2$) and stored at room temperature. The incubation water was exchanged with new start water and the next incubation phase was started.

Salinity and differences in reactor weight were recorded to account for possible evaporative losses during incubation, as evaporation influences TA (Zeebe & Wolf-Gladrow, 2001).

2.5 Applied Methods and Measurements

According to the study question, we applied methods to determine calcification rates (via buoyant weight and total alkalinity technique) and photosynthetic performance (via O_2 evolution and consumption) in response to the applied treatment. Nutrient measurements were applied to control experimental conditions.

2.5.1 Nutrient Determination according to Seal Analytical

The inorganic nutrients nitrite (NO_2^-), nitrate (NO_3^-), phosphate (PO_4^{3-}) and silicate (Si) were measured with a nutrient autoanalyzer (Seal Analytical, CFA Quaatro) according to Seal Analytical (NO_2^-: method no. Q-070-05, NO_3^-: method no. Q-068-05, PO_4^{3-}: method no. Q-064-05, Si: method no. Q-066-05). Detection limits were $\pm$ 0.01, 0.03, 0.01 and 0.02 μmol l^{-1} for NO_2^-, NO_3^-, PO_4^{3-}

and Si, respectively. Measurements were single determinations.

In case of measured negative NO_2^-, NO_3^-, PO_4^{3-} or Si concentrations, the most negative value was set to zero and its difference to zero was added to all other values. For each incubation phase the difference between start and end concentrations was calculated and considered as algal uptake, resulting in uptake rates for each incubation phase. Uptake of dissolved inorganic nitrogen (ΣN) was calculated from pooled NO_2^- and NO_3^- concentrations. Algal uptake was corrected for concentration differences measured in the blank of corresponding treatment combination. Relative consumptions rates were calculated according to (eq. 8) with X_{rel} = relative uptake of NO_2^-, NO_3^-, PO_4^{3-} and Si in each reactor, $X_{net\ (treatment)}$ = absolute uptake of NO_2^-, NO_3^-, PO_4^{3-} and Si in each reactor during the treatment phase and $X_{net\ (baseline)}$ = absolute uptake of NO_2^-, NO_3^-, PO_4^{3-} and Si in each reactor during the mean baseline phase.

2.5.2 pH

pH (NBS scale) was measured with a portable pH meter (Metrohm, 826pH, precision ± 0.01 units) in all reactors directly after opening the lid. Reactors were measured in the sequence of their pCO_2 level, starting with the lowest level in order to minimize the equilibration time of the pH probe. Each measurement took about 4 minutes until pH readings were constant. The pH probe was regularly calibrated (NBS scale) with buffer solution (Metrohm Ion Analysis) and corrected against certified reference material for ocean carbonate measurements (Prof. A.G. Dickson, Marine Physical Laboratory, University of California).

Measured pH raw data were corrected for actual temperature and certified reference material using eq. 10 according to Dickson *et al.* (2007). pH (NBS scale) was thereby converted to pH (total scale) (pH_T).

$$pH_T(sample) \;=\; pH_T(ref) + \frac{\left[\left(\frac{measured\ pH_{NBS}}{1000}\right)_{ref} - \left(\frac{measured\ pH_{NBS}}{1000}\right)_{sample}\right]}{\left[R * (T + 273.15K) * \left(\frac{Ln10}{F}\right)\right]} \tag{10}$$

with T = temperature at measurement (°C), R = Revelle factor: 8.315, F = Faraday constant: 96485.340 (C mol^{-1}). pH_T (ref) referred to the pH of the reference material (Dickson batch 108, 2011) calculated for the total scale and 20°C from according TA, DIC, salinity, Si and PO_4^{3-} by using the software CO2SYS (Lewis & Wallace, 1998) and following constants: KSO_4 from Dickson, and K_1 and K_2 from Mehrbach *et al.* (1973), refitted by Dickson & Millero (1987).

2.5.3 Carbonate System

Carbonate system parameters pCO_2 and carbonate saturation state for calcite (Ω_{Ca}) and aragonite (Ω_{Ar}) were calculated for each replicate with the software CO2SYS (Lewis & Wallace, 1998) from pH_T and total alkalinity (TA), salinity, temperature, PO_4^{3-} and Si (Riebesell et al., 2010). We used the constants KSO_4 from Dickson, K_1 and K_2 from Mehrbach *et al.* (1973), refitted by Dickson & Millero (1987). For pH_T and temperature we used individual measured values, for TA and salinity a mean of start values (2366.5 ± 23.6 μmol kg^{-1}, 30.4 ± 0.1), for PO_4^{3-} and Si a mean concentration of 0.140 and 0.030 μmol l^{-1}, respectively.

2.5.4 Buoyant Weight Measurements according to Davies (1989)

The buoyant weighing technique is a non-destructive way to measure the calcium carbonate ($CaCO_3$) amount of living calcified organisms (Davies, 1989). This method was originally established for coral studies (Jokiel *et al.*, 1978), but was also applied to coralline algae (Potin *et al.*, 1990, Jokiel *et al.*, 2008, Martin & Gattuso, 2009, Ries *et al.*, 2009). We used the technique to measure growth and calcification of incubated alga specimens: as the amount of $CaCO_3$ in *L. glaciale* varies between 80 - 90% of total biomass (Bilan & Usov, 2001), $CaCO_3$ deposition (calcification) takes a significant part in growth. Therefore, $CaCO_3$ deposition and growth can be regarded as equivalent in *L. glaciale*.
The key idea of the buoyant weight method is, that organic material, e.g. tissue, has approximately the same density as sea water, whereas mineralized structures, e.g. calcified tissue, have a higher density than sea water. Consequently, by weighing living specimens under water only the weight of included mineralized structures, like $CaCO_3$, contributes to the buoyant weight (Jokiel *et al.*, 1978). An increase in specimen's weight over time gives the increase in $CaCO_3$ over time, indicating calcification.
From a measured buoyant weight the weight in air is calculated with eq. 11. The density of the actual object can be calculated by rearranging eq. 11, see eq. 12:

$$Weight\ of\ object\ in\ air\ =\ \frac{Wt_W}{1-\frac{D_W}{D_O}} \tag{11}$$

$$Density\ of\ object\ =\ \frac{D_W}{1-\frac{Wt_W}{Wt_A}} \tag{12}$$

with Wt = weight of object, W = water, A = air, D = density, O = object.

In order to determine the buoyant weight of our alga specimens we used an electronic scale (Sarto-

rius, CPA225D, precision ± 0.01 mg), which was mounted on a water bath filled with start water. A weighing platform was immersed into the water bath and connected with the scale by a wire (fig. 7). The wire was made of wolfram in order to reduce water adhesion, possibly inferring with the weighing process. Air bubbles adhering to the platform or the wire were removed.

Salinity and temperature were constantly recorded during weight measurements with a combined salinity probe (Metrohm, WTW TetraCon 325 with WTW Multi 350i device) in order to correct for water density changes. Weight measurements were carried out at constant temperatures of 15°C and during measurement the water bath was covered with a piece of styrofoam in order to ensure constant measurement conditions. A reference object of known density (glass: 2.5 g cm^{-3}) was weighted at the beginning and the end of each measuring day and whenever temperature or salinity changed by 0.1 unit.

Precise weight determination was done with the 100 point measurement mode of the scale: the reference object or alga specimen was placed on the under water platform (fig. 8) and automatically weighted 100 times. The scale weight output was the mean of the 100 measurements, being a representative weight of the measured object or alga specimen. Weight measurements were repeated at least once per object, precision was within ± 0.001 g. All alga specimens were measured before and after the experiment.

For density determination of algal $CaCO_3$, 10 specimens were bleached in a 10% solution of sodium hypochloride (NaClO), dried and subsequently weighted in air (Sartorius, BP310P, precision 0.001 g) and water (buoyant weight). In order to obtain constant buoyant weights of dried specimens, these had to be placed in water some time ahead of weighing, because they absorbed water and it took some time until they were water saturated.

Water density was calculated with recorded salinity and temperature data and respective software (Tomczak, 2000 based on Fofonoff & Millard, 1983). Calcite density was calculated with eq. 12. By using water density, mean algal calcite density and the measured buoyant weights, the weight of each algal specimen in air was calculated with eq. 11. Production of $CaCO_3$ over the experimental duration was calculated from the difference between start and end buoyant weight of individual alga specimens.

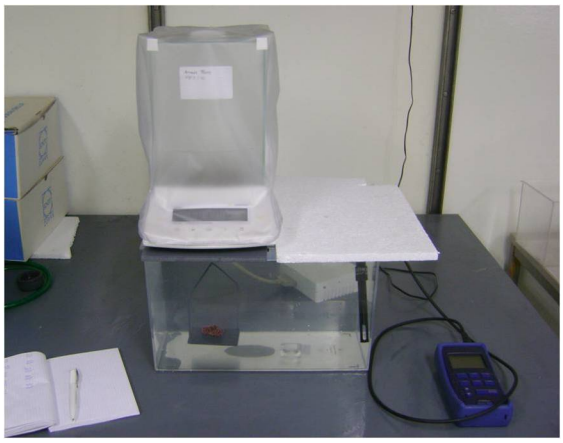

Figure 7: Buoyant weight measurement set-up: An electronic scale was mounted on a water bath with the weighing platform connected to the undersite of the scale. The styrofoam covering should reduce water motion in order to ensure constant measurements. Salinity and temperature were recorded with a combined probe.

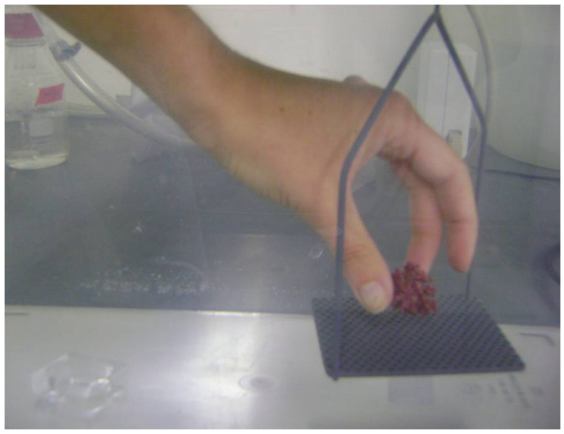

Figure 8: Underwater platform of the buoyant weighing scale. The platform was connected by wire to the underside of the scale. The wire was made of wolfram in order to reduce water adhesion, likely influencing the measurement. For weight measurements specimens were placed carefully onto the platform as shown in the picture.

2.5.5 Total Alkalinity Determination according to Dickson *et al.* (2003)

Total alkalinity (TA) was determined via open-cell acidimetric titration with an automatic titration device (Metrohm, Titrando 808) and 0.005 N hypochloric acid (HCl). A subsample of 10 ml was extracted with a syringe, weighted (Sartorius, RC210D, precision 0.0001 g) in order to determine its exact volume, 0.2 μm filtered and titrated. Samples were measured at least twice, precision was $\pm$ 0.005 μmol kg^{-1}. Samples were corrected with certified reference material for ocean carbonate measurements (Prof. A.G. Dickson, Marine Physical Laboratory, University of California). The electrode was calibrated with a three point calibration and buffer solution (Roth) every third day. TA was calculated with a non linear curve fitting algorithm based on the Gran function, implemented in a Matlab script (according to Dickson *et al.*, 2003).

TA measurements of the sampled water were corrected for the exact water volume and changes in salinity. Changes in TA during incubation time (difference between start and end value of each incubation phase) were used to calculate net calcification rates. According to Smith & Key (1975), calcification and TA concentrations are in a stoichiometric relationship: calcification lowers TA by two equivalents for one mole precipitated $CaCO_3$ (eq. 3). Therefore, changes in TA concentrations allow the precise calculation of calcification rates, if calcification is the only possible process affecting TA concentrations. Possible other processes affecting the TA concentrations have to be excluded from the system or have to be corrected for (e.g. nutrient concentration changes). Relative calcification rates were calculated according to (eq. 8) with X_{rel} = relative calcification (%), $X_{net\ (treatment)}$ = absolute

calcification during the treatment phase, and $X_{net\ (baseline)}$ = absolute calcification during the mean baseline phase.

2.5.6 Optode-Based Photosynthetic and Respiratory O_2 Measurements

Photosynthetic O_2 evolution and respiratory O_2 consumption under the experimental treatment were measured with optical electrodes (optodes) via changes in O_2 concentrations in light and dark in the surrounding medium, indicating photosynthetic performance. The experimental set-up was established by Form (2011) in collaboration with the Institute for Polar Ecology (IPÖ) Kiel. Measurements of O_2 concentrations followed every other incubation phase. The first measurement of O_2 concentrations was conducted under baseline conditions (target values: 390 μatm, 3.5°C) following the general experimental design (2.2).

Principle of Optical Sensing of Oxygen according to PreSens (2005)

Applied O_2 measurements were based on the dynamic quenching of luminescence by molecular oxygen. The absorption of light elevates luminescent indicator molecules (luminophores) into an excited state, where they emit the gained energy in form of luminescence. When luminophores collide with other molecules while being excited, they transfer their energy to the colliding molecule, themselves being deactivated without emitting light (dynamic quenching). The decrease in luminescence is measurable; its decay time in the presence of O_2 is a function of O_2 concentration according to the Stern-Volmer-Equation (eq.13):

$$\frac{L_0}{L} = \frac{R_0}{R} = 1 + K_{sv} * O_2 \tag{13}$$

with L_0 = luminescence intensity in the absence of oxygen, L = luminescence intensity in the presence of oxygen , R_0 = luminescence decay time in the absence of oxygen, R = luminescence decay time in the presence of oxygen, K_{sv} = Stern-Volmer constant, $[O_2]$ = oxygen concentration.
We used a 10-channel fiber-optic oxygen meter (PreSens, OXY-10), which regularly excited respective luminophores embedded in sensor spots (optodes) (PreSens) by sinusoidal lightning. Thereby, luminescence decay time was measured by phase modulation: at decay, the luminescence signal is delayed in time and consequently in sinus phase, i.e. decay time is expressed in phase angle between excited state (lightning) and luminescence signal. As the decay time is a function of prevailing O_2 concentration so is the measured phase angle.

Measurement Set-Up

The set-up for the measurements of O_2 concentrations consisted of a water baths and eight independent oxygen incubation chambers (fig. 9). To establish experimental treatment temperatures in the water bath, a flow through cooling system was established: water from the water bath was drained into a reservoir bath of similar size, which fed into a cooling aggregate (Aqua Medic, Titan 4000). Cooled water out of the aggregate was pumped back into the water bath. The water circulation was driven by means of a pump (Eheim Universal). To reduce the hysteresis effect of the cooling device on the water temperature, water in the reservoir bath was heated by a titanium immersion heater (Schego, 300W). Heating sped up the warming process of the water and therefore increased the cooling intervals per time, increasing the total time at applied target temperatures. The immersion heater was controlled by a computer (IKS, Aquastar). Cooling aggregate and immersion heater were adjusted in such a way, that target temperature levels within the water bath could be met. Temperatures were logged (PreSens, F1Box). A streaming pump (Hydor, Koralia 1, 1500 l h^{-1}) accounted for water current and mixing in the water bath. The light regime was adjusted with two blue fluorescent lamps (Arcadia, Marine Blue 420 nm Actinic T5), which were placed above the water bath and darkened with grey foil to the desired underwater irradiance of 12 μmol photons m^{-2} s^{-}, according to the main experiment. Underwater irradiance was controlled with a light meter (Licor, Li-250A).

Independent oxygen incubation chambers were of cylindrical shape and made of acryl glass. They enclosed a water volume of 875 ml (without content) and were air tight. Incubation chambers contained a small table, where organisms were placed on, and a magnetic stir bar under the table, establishing a water current. The magnetic stir bars were driven by a low voltage electric motor which was controlled by an external multi channel transformer. A planar O_2 optode (PreSens, SP-PSt3-NAU-D7-YOP) was placed at the inner side of each lid (compare fig. 10, 11). Optodes were activated by light impulses from glass fibre wires from the outer side of the lid. Subsequent O_2 concentrations were measured with a ten channel oxygen meter (PreSens) according to the principle of optical sensing of O_2 (PreSens). The oxygen meter was connected to a standard computer, recording the measurement with respective software (PreSens, OXY 10v3-33FB) (compare Form, 2011).

Measurement

Before the start of O_2 measurements, optodes were calibrated for each temperature level against 100% and 0% O_2 according to PreSens (2005)(two-point calibration). O_2 saturated water was obtained by aeration of water with ambient air. O_2 free water was obtained by mixing water with a supersaturated solution of sodium sulphite (Na_2SO_3). The calibration was recorded by the OXY 10v3-33FB software.

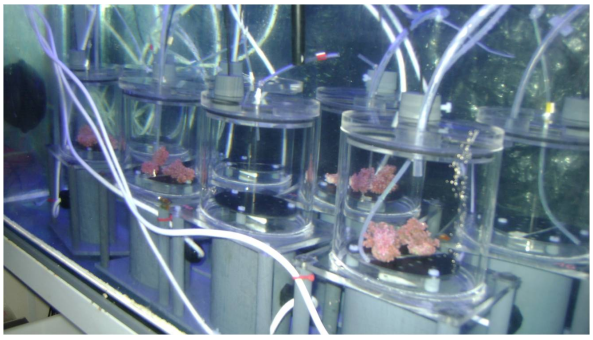

Figure 9: Incubation chambers for O_2 measurements, submersed in the water bath during measurement. Each two chambers were assigned to one CO_2 level: one chamber contained all four alga specimens of the respective treatment combination, the other chamber stayed empty, serving as blank to monitore O_2 changes in the incubation.

O_2 measurements comprised a light (two days) and a dark (one day) phase, in order to measure light and dark O_2 changes. The light phase referred to Arctic summer light conditions.

O_2 measurements were conducted separately for all temperature levels. For each temperature, two incubation chambers were assigned to one CO_2 level: one chamber was filled with all four alga replicates of one treatment combination (2.2), the other chamber was without alga specimens and served as blank, recording oxygen changes in the incubation water, e.g. due to microbial activity. Incubation chambers were filled with filtered, CO_2 pre-equilibrated water according to the corresponding treatment (compare 2.4). Lids were closed air tight without enclosing air bubbles. The O_2 concentration within the chambers was measured every 15 seconds based on optical sensing, first in light and subsequently in dark without stopping the measurement. After three days the O_2 measurement was stopped and algae were exchanged.

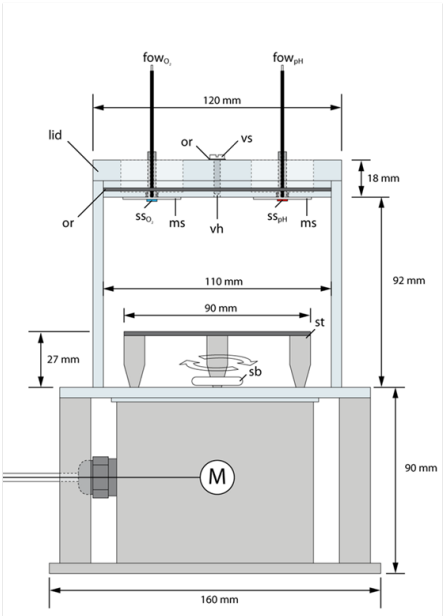

Figure 10: Incubation chamber for O_2 measurements, schematic drawing (A. Form). See the sensor spot (ss_{O2}) attached at the inner side of the lid.

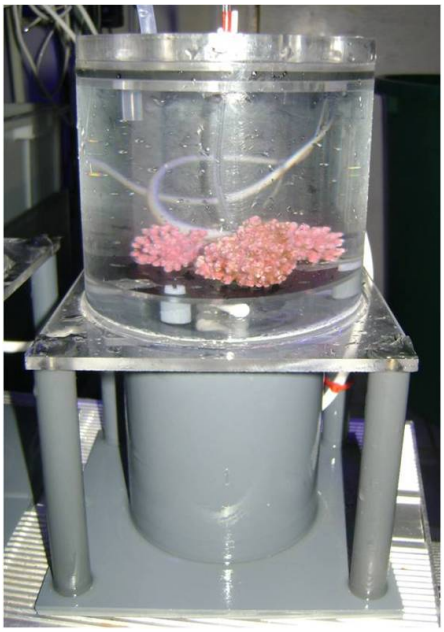

Figure 11: Incubation chamber with four algae specimens, prepared for O_2 measurements.

The raw data of O_2 concentrations measured within the incubation chambers was divided into light and dark phase. Since the slope of change in O_2 concentrations over the measuring time was constant, i.e. O_2 evolution in light increased linearly and O_2 consumption in the dark decreased linearly, respective rates were considered constant. In order to calculate O_2 evolution and consumption rates for algae groups of each treatment combination, the change of O_2 concentration for the period of 1 day was used.

Concerning the solubility of oxygen in water, respective O_2 concentrations per day and algae group were corrected for calibration values, air pressure at the time of measurement (obtained from regular measurements at the roof of GEOMAR, research unit Marine Meteorology) and recorded temperature during measurement. Absolute O_2 concentrations in μmol h^{-1} were calculated with respect to actual and standard air pressure, partial pressure (O_2 and water vapour), volume content of O_2 in air, salinity compensated Bunsen absorption coefficient, molecular mass and molar volume of O_2, water volume of the incubation chambers and incubation time in hours (for more detail see Form, 2011).

Relative O_2 evolution, respectively consumption rates were calculated from obtained absolute rates by using eq. 8 with X_{rel} = relative O_2 evolution/consumption (%), $X_{net\ (treatment)}$ = absolute O_2 evolution/consumption during the treatment phase, and $X_{net\ (baseline)}$ = absolute O_2 evolution/consumption during the mean baseline phase.

2.6 Applied Statistics

Statistical evaluation of results was done with the software Statistica 8. The applied treatment factors "elevated pCO_2" and "elevated temperature" (target levels as categorical factors) were tested for their statistical significant effects on difference in nutrient uptake, buoyant weight, relative net calcification rates, and relative net O_2 production and respiration rates. The general null hypothesis was that there would be no single or combined effect of the applied factors. Following statistical tests were applied: a two-factorial analysis of variance (MANOVA) for differences in buoyant weight and relative net calcification rates, and a multiple regression analysis for relative nutrient uptake and relative net O_2 production and respiration rates. The regression analysis accounted for a low replicate number of nutrient uptake rates and O_2 rate measurements per treatment combination (only 1 replication, i.e. two data points per combination). All data were tested for assumptions of the respective statistics, i.e. normal distribution (Shapiro-Wilks test) and homogeneous variances (Levene's test). Following the main statistical tests a post-hoc test (LSD test) was conducted to find out about significant effects between single combinations.

3 Results

3.1 Identification

For genus and species identification of collected algal material three randomly chosen algae individuals were taxonomically identified following recommondations for crustose coralline algae given in Woelkerling (1988). Diagnostic key features of rhodolith-forming genera (Harvey & Woelkerling, 2007) were compared to SEM pictures of algae specimens. Following key features were positively identified on algal SEM pictures: epithallial cells with flattened and flared outermost cell walls, cell-fusions and no secondary pit-connections. Flared epithallial cell walls and cell fusions were identified in vertical (fig. 12), respectively horizontal (fig. 13) sections. Secondary-pit connections could not be identified. Among rhodolith-forming coralline alga genera the combination of no secondary pit-connections and flared epithallial cells is present only in *Lithothamnion* (Melobesioideae, compare 1.3) (Harvey & Woelkerling, 2007).

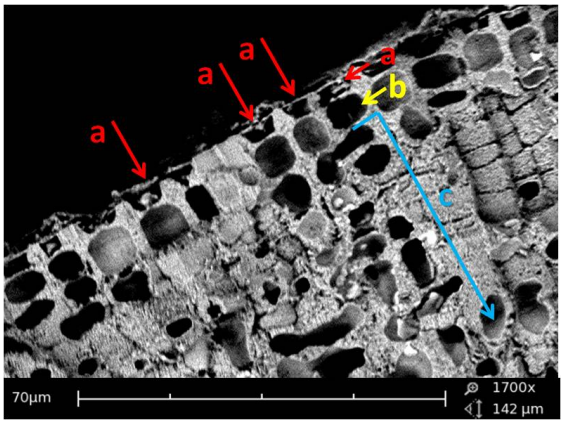

Figure 12: Vertical section of *Lithothamnion glaciale* from Kongsfjorden, Svalbard, Norway. a. Flat and flared epithallial cells in the outermost cell layer (epithallium) b. Meristematic cells below the epithallium (intercalary meristem) c. Vegetative cells of the perithallium. SEM (Phenom G2 pure desktop) GEOMAR, Kiel.

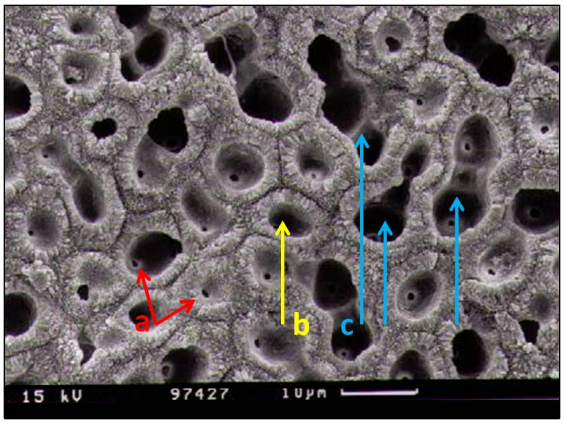

Figure 13: Horizontal section of *Lithothamnion glaciale* from Kongsfjorden, Svalbard, Norway. a. Primary pit-connections b. Calcified cell walls c. Cell fusions. SEM (CamScan 44/EDX) Institute for Geosciences, Kiel.

Three species of the genus *Lithothamnion* are described for Spitzbergen according to Hansen & Jenneborg (1996) and Guiry & Guiry (2012): *L. flavescens*, *L. glaciale* and *L. tophiforme*. One diagnostic feature to differentiate between these species is the mean surface cell diameter (fig. 14) (Adey *et al.*, 2005). The mean surface cell diameter of our specimens was 8.51 $\pm$ 0.6 μm (7.03 - 10.00 μm) which is in the range of values reported for *L. glaciale* of 8.0 $\pm$ 1.14 μm (Adey *et al.*, 2005). The mean surface cell diameter of *L. tophiforme* is 11.7 $\pm$ 1.15 (Adey *et al.*, 2005). Mean surface cell diameters of *L. flavescence* are not reported so far.

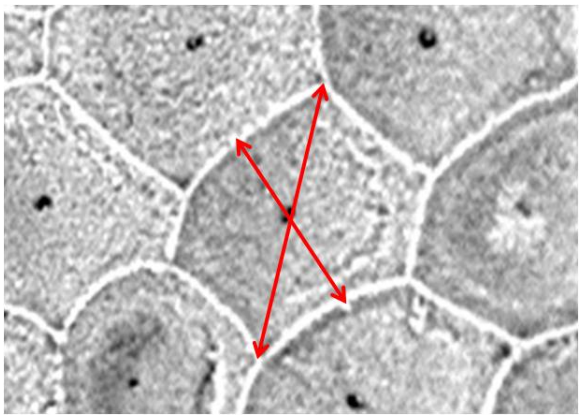

Figure 14: Epithallial cell surfaces of *L. glaciale* from Kongsfjorden, Svalbard, Norway.
The longest and shortest distance of a surface cell, running through the pit-plug until the cell membrane (red arrows), was used as diagnostic feature for species identification of *L. glaciale*. SEM (Phenom G2 pure desktop) GEOMAR, Kiel.

Following the taxonomic keys and species descriptions for Arctic crustose coralline algae (Hansen & Jenneborg, 1996; Adey *et al.*, 2005; Harvey & Woelkerling, 2007; Guiry & Guiry, 2012) our collected and identified alga specimens are of the species *L. glaciale* Kjellman, 1883. *L. glaciale* is described to be a dominant species of the benthic habitat in the Subarctic, including Spitzbergen (Adey *et al.*, 2005; Hansen & Jenneborg, 1996).

3.2 Photo Database

The photo database comprised front- and backside pictures of all experimentally used alga specimens both before and after the experiment. By comparing pre- and post-experimental pictures, changes in surface colour and texture of incubated coralline algae could be visually analysed after the experiment (fig. 15). Post-experimental pictures showed a brown film on the surface of all algae (see fig. 15(b)) as well as abundant white spots (see fig. 15(d)). The brown film was not identified and the abundance of white spots was not qualitative assessed. A subjective impression revealed no tendency regarding the applied treatment.

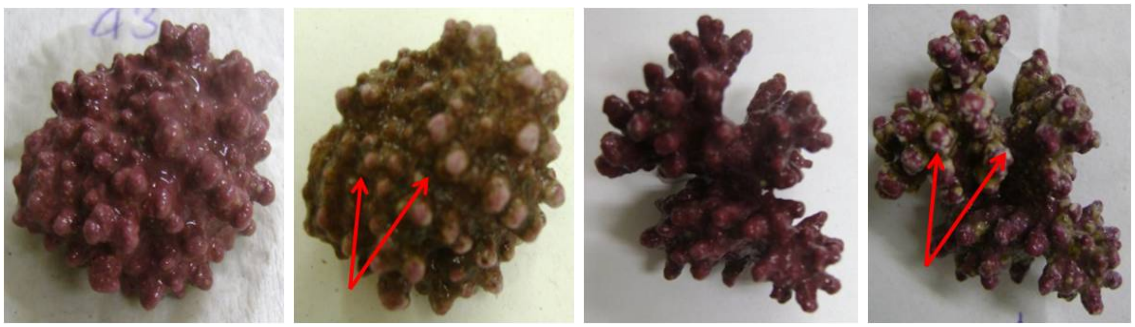

((a)) no. 1 pre-exp. ((b)) no. 1 post-exp. ((c)) no. 48 pre-exp. ((d)) no. 48 post-exp.

Figure 15: Representative pre- and post-experimental pictures of experimentally used *L. glaciale*. Treatment conditions for alga no. 1 and alga no. 48 were 7.5 ± 0.1°C and 1518 ± 136 μatm, respectively 3.4 ± 0.1°C and 569 ± 48 μatm. Fig. 15(a) and fig. 15(c) show *L. glaciale* before, fig. 15(b) and fig. 15(d) after experimental incubation. Red arrows indicate an observed brown film (fig. 15(b)), respectively white spots (fig. 15(d)) on algae surfaces.

3.3 Applied Treatment and Light Regime

The applied CO_2 treatment did not meet our expectations in regard to aimed target levels; the applied temperature treatment and light regime did meet our expectations. Applied CO_2 treatment levels calculated from pH and total alkalinity (TA) measurements were higher than aimed target levels (tab. 2). In comparison to target levels, the lowest CO_2 level had a mean offset of nearly 180 μatm, all elevated CO_2 levels had a mean offset of 380 $\pm$ 20 μatm. The four CO_2 levels were still distinct as standard deviations did not overlap. Resulting mean level pCO_2 were 569 $\pm$ 48, 920 $\pm$ 86, 1230 $\pm$ 120 and 1518 $\pm$ 136 μatm.

Applied temperature treatment levels were with 3.4 $\pm$ 0.1, 5.2 $\pm$ 0.1 and 7.5 $\pm$ 0.1 °C close to target levels. Mean underwater irradiances at the bottom of each water bath were 11.62 $\pm$ 0.81, 12.95 $\pm$ 1.36 and 12.1 $\pm$ 1.13 μmol photons m^{-2} s^{-1} for temperature levels of 3.4, 5.2 and 7.5°C, respectively. The variation in irradiance between temperature levels (freezer cabinets) was 8.2 $\pm$ 1.8 %. Underwater irradiance was measured at the same depth as algae were located within the reactors. Mean underwater irradiance was close to the target level of 12 μmol photons m^{-2} s^{-1}. Irradiance decreased over the experimental duration by $\sim$ 1.17 μmol photons m^{-2} s^{-1} in all freezer cabinets.

3.4 Nutrient Uptake

The difference between start and end concentrations of measured Si, PO_4^{3-}, NO_2^- and NO_3^- was calculated for each incubation period and regarded as uptake. Uptake of dissolved inorganic nitrogen (ΣN) was calculated from pooled NO_2^- and NO_3^- concentrations. Relative uptake relates to uptake under ambient control conditions (baseline), according to eq. 8.

Si concentrations remained constant at 0.110 $\pm$ 0.054 μmol kg^{-1} over the experimental duration. PO_4^{3-} concentrations were overall low with mean start concentrations of 0.03 $\pm$ 0.02 μmol kg^{-1} close to the detection limit of 0.01 μmol kg^{-1}. Significant changes during the incubation period could not be identified.

Relative uptake of ΣN increased over experimental duration with the highest mean relative uptake of 262 $\pm$ 132% after the third treatment phase (fig. 16). Relative uptake of ΣN decreased significantly with increasing temperature (p-value = 0.00). The highest mean relative uptake of ΣN was measured at 3.4°C. Mean relative uptake of ΣN at 5.5°C and 7.5°C was $\sim$ 30%, respectively $\sim$ 26% lower than at 3.4°C (fig. 17). Relative uptake of ΣN at 7.5°C had large standard deviations, which ranged from $\sim$ 40% to $\sim$ 300% (fig. 17). Elevated CO_2 had no effect on uptake of ΣN.

Data were normally distributed (Shapiro-Wilks test) after root-transformation. We found a statistical significant effect of elevated temperature on uptake of ΣN (compare tab. 3)

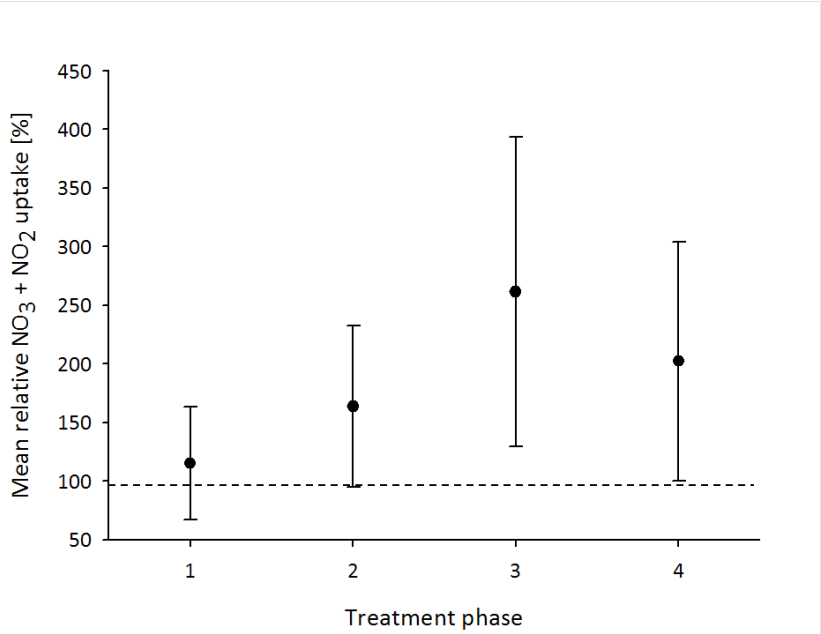

Figure 16: Mean relative uptake of ΣN of *L. glaciale* over treatment duration. Datapoints are means of pooled CO_2 and temperature treatments (12 combinations with each 2 measurements) from each one treatment phase. Standard deviations (± SD) are plotted against treatment duration (time). Relative rates are normalized to rates of each individual alga under ambient conditions (3.4 ± 0.1°C, 568 ± 41 μatm: baseline). The black dashed reference line at 100% indicates the baseline rate.

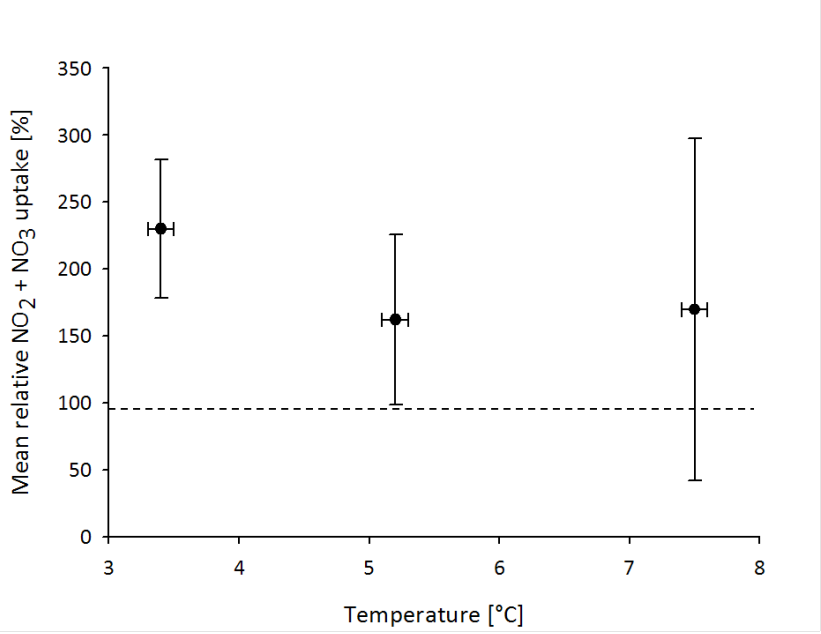

Figure 17: Mean relative uptake of ΣN of *L. glaciale* with temperature. Data points are means of pooled CO_2 treatment (4 CO_2 levels with each 2 measurements) from four treatment phases. Standard deviations (± SD) are plotted against the applied temperature treatment. Horizontal error bars give the SD of the temperature over the experimental duration. Relative rates are normalized to rates of each individual alga under ambient conditions (3.4 ± 0.1°C, 568 ± 41 μatm: baseline). The black dashed reference line at 100% indicates the baseline rate.

Table 2: Carbonate system parameters were calculated with CO2SYS from pH_T (total scale) and total alkalinity (TA) measurements, temperature (T) and salinity (S). Data are the means of 16 (S), 360 (T), 18 (TA), 360 (pH_T) replicates. Calculated parameters are CO_2 partial pressure (pCO_2) in μatm, carbonate saturation state for calcite (Ω_{Ca}) and aragonite (Ω_{Ar}), each ± SD, for actual temperatures 3.4 ± 0.1, 5.2 ± 0.1, 7.5 ± 0.1°C.

Target levels		S	T	TA	pH_T	pCO_2	Ω_{Ca}	Ω_{Ar}
			(°C)	(μmolkg^{-1})		(μatm)		
T (°C)	pCO_2 (μatm)							
3.5	390	30.4 ± 0.1	5.0 ± 0.9	2366.5 ± 23.6	7.89 ± 0.02	568 ± 41	1.85 ± 0.11	1.16 ± 0.07
	560		5.1 ± 0.8		7.67 ± 0.04	993 ± 86	1.15 ± 0.10	0.72 ± 0.06
	840		4.6 ± 0.7		7.55 ± 0.04	1346 ± 110	0.87 ± 0.08	0.54 ± 0.05
	1120		5.0 ± 0.5		7.46 ± 0.04	1654 ± 112	0.71 ± 0.05	0.45 ± 0.03
5.5	390	30.4 ± 0.1	5.9 ± 1.4	2366.5 ± 23.6	7,90 ± 0,02	583 ± 59	1.98 ± 0.14	1.24 ± 0.09
	560		6.5 ± 0.6		7.72 ± 0.03	886 ± 55	1.37 ± 0.08	0.86 ± 0.05
	840		6.6 ± 0.5		7.60 ± 0.02	1195 ± 52	1.05 ± 0.04	0.65 ± 0.03
	1120		6.4 ± 0.9		7.51 ± 0.01	1479 ± 93	0.86 ± 0.05	0.54 ± 0.03
7.5	390	30.4 ± 0.1	8.4 ± 0.9	2366.5 ± 23.6	7.93 ± 0.04	556 ± 70	2.29 ± 0.22	1.44 ± 0.14
	560		8.3 ± 1.0		7.74 ± 0.02	881 ± 65	1.54 ± 0.10	0.96 ± 0.06
	840		8.3 ± 0.7		7.64 ± 0.03	1149 ± 85	1.21 ± 0.08	0.76 ± 0.05
	1120		8.6 ± 0.6		7.54 ± 0.02	1422 ± 70	1.00 ± 0.04	0.63 ± 0.03

3.5 Carbonate System

The calculated carbonate system parameters pCO_2 (μatm) and saturation state (Ω) for calcite and aragonite are given in table 2. All actual pCO_2 levels were higher than target levels (compare 3.3). pCO_2 was highest at the lowest temperature (3.4 °C) and lowest at the highest temperature (7.5 °C). CO_2 levels were distinct. The lowest CO_2 level (target 390 μatm) was at all temperature levels supersaturated with respect to Ω_{Ar}. All elevated CO_2 levels were undersaturated at all temperature levels with respect to Ω_{Ar}. For Ω_{Ca} the two high CO_2 levels (target 840 and 1120 μatm) were undersaturated for 3.4°C and for the highest CO_2 level also at 5.2°C. All other CO_2 levels were supersaturated with respect to Ω_{Ca} at all temperature levels.

3.6 Calcification

Net calcification was measured via the increase in algal calcium carbonate ($CaCO_3$) content (buoyant weight technique (Davies, 1989)) and via changes in water chemistry (total alkalinity technique (Smith & Key, 1975)). Net calcification rates were in good agreement between both methods (fig. 19, 18). Net calcification rates obtained from both methods were highest at the two lower pCO_2 levels and were

decreased with increasing pCO_2. Net calcification at 3.4°C was nearly constant at all pCO_2 levels and was decreased with increasing pCO_2 levels at 5.2°C. Net calcification at 7.5°C was increased at the two lower pCO_2 levels and was decreased at the two higher pCO_2 levels.

Net calcification rates obtained from the buoyant weight technique were positive at all temperature and pCO_2 levels, as well as two to four times higher and with larger standard deviations than net calcification rates calculated with the total alkalinity technique. Net negative calcification in the highest pCO_2 at 7.5°C was only visible in calcification rates calculated from the total alkalinity technique.

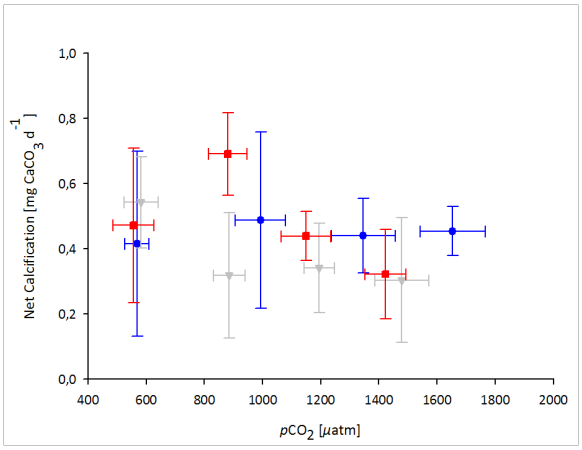

Figure 18: Net calcification of *L. glaciale* with pCO_2, measured with the buoyant weight technique (Davies, 1989). Data points are means (n = 4) of each temperature treatment (blue = 3.4°C, grey = 5.2°C, red = 7.5°C). Standard deviations (± SD) are plotted against pCO_2; horizontal error bars give the SD of the pCO_2 over the experimental duration.

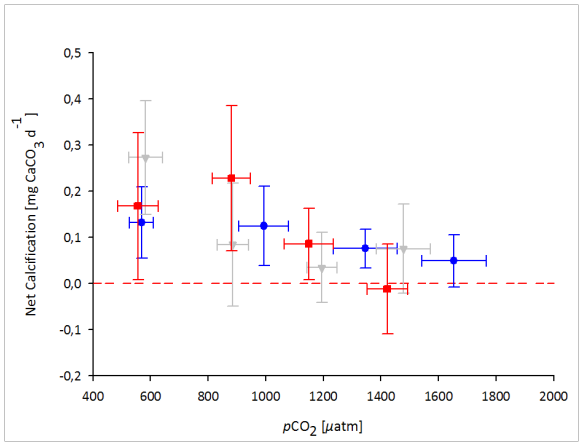

Figure 19: Net calcification of *L. glaciale* with pCO_2, measured with the total alkalinity technique (Smith & Key, 1975). Data points are means (n = 24) of each temperature treatment pooled for the experimental duration (blue = 3.4°C, grey = 5.2°C, red = 7.5°C). Standard deviations (± SD) are plotted against pCO_2; horizontal error bars give the SD of the pCO_2 over the experimental duration. The red dashed reference line at 0.0 mg $CaCO_3$ d^{-1} indicates zero calcification; negative calcification (dissolution) occures below 0.0 mg $CaCO_3$ d^{-1}.

3.6.1 Buoyant Weight

The $CaCO_3$ content in mg individuum^{-1} of each alga was calculated from measured buoyant weight according to eq. (11). The density of algal calcite was 2.378 g cm^{-3} ± 0.288 g cm^{-3}, which was close to the calcite density measured in *L. glaciale* from the Kattegatt of 2.645 g cm^{-3} (A. Form, personal communication). $CaCO_3$ weight increased over the experimental duration, indicating net calcification in all algae. The mean increase in $CaCO_3$ weight ($CaCO_3$ precipitation) was slightly higher at the two lower pCO_2 levels compared to the two higher pCO_2 levels (fig. 20). Mean $CaCO_3$ precipitation at 569 and 920 μatm was 76 ± 42 mg and 68 ± 34 mg, respectively. Mean $CaCO_3$ precipitation at 1230 and 1518 μatm was 50 ± 14 mg and 51 ± 25 mg, respectively. Looking at the different temperature

levels, mean $CaCO_3$ precipitation at 3.4°C was constant with increasing pCO_2. At 5.2°C mean $CaCO_3$ precipitation was highest at lowest pCO_2 and constant lower with increasing pCO_2. At 7.5°C mean $CaCO_3$ precipitation was high at the two lower pCO_2 and was decreased with increasing pCO_2 (fig. 19).

Data were normally distributed (Shapiro-Wilks test) after root-transformation (see tab. 3). We found no statistical significant effect of elevated temperature or CO_2 on net calcification (compare tab. 3). Standard deviations of mean $CaCO_3$ precipitation with pCO_2 level were overlapping.

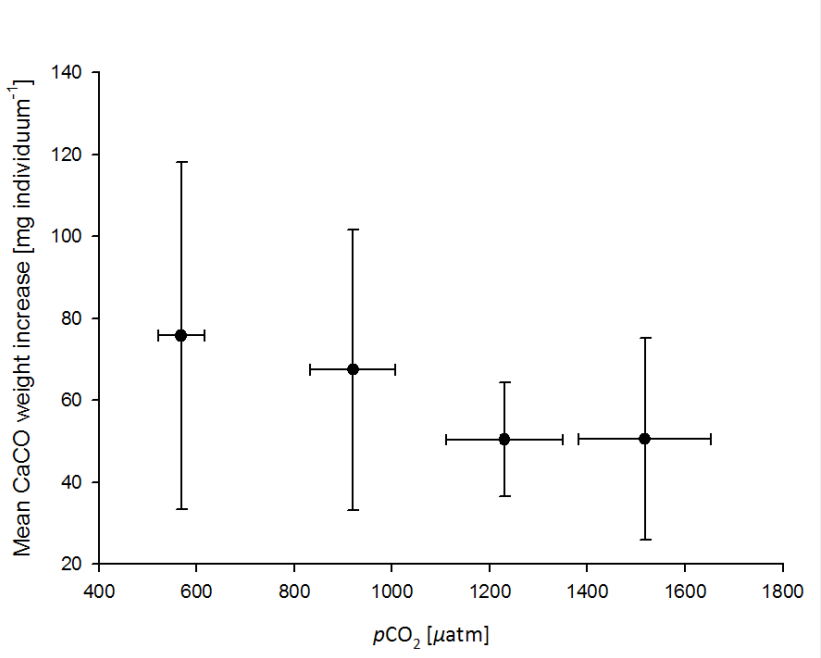

Figure 20: Mean $CaCO_3$ precipitation of *L. glaciale* with pCO_2, measured with the buoyant weight technique (Davies, 1989). Data points are means of the pooled CO_2 treatment (n = 12). Standard deviations (± SD) are plotted against pCO_2; horizontal error bars give the SD of the pCO_2 over the experimental duration.

3.6.2 Total Alkalinity

Net calcification rates of *L. glaciale* were calculated with the total alkalinity technique (Smith & Key, 1975). Mean net calcification was decreased with increasing pCO_2 level; the decrease in mean net calcification was different between temperature levels (fig. 19) as described in 3.6.

Relative calcification (%) was calculated according to eq. 8. Mean relative calcification decreased over experimental duration at all temperature levels (fig. 21). Mean relative calcification at 3.4°C and 5.2°C decreased until the third treatment phase to 29 ± 25% and 46 ± 143%, respectively, and increased slightly in the fourth treatment phase; mean relative calcification was reduced compared to

the baseline but positive. Mean relative calcification at 7.5°C increased compared to the baseline until the second treatment phase, and decreased in the subsequent treatment phases. In the last treatment phase (after 8 weeks treatment), mean relative calcification at 7.5°C was zero, i.e. by 100% reduced to baseline calcification.

Mean relative calcification was decreased with increasing pCO_2 levels, being higher at 569 μatm and 920 μatm than at 1230 μatm and 1518 μatm. At 1518 μatm mean relative calcification was negative. Looking at the temperature levels, mean relative calcification at 3.4 °C was reduced at all pCO_2 levels (49 $\pm$ 21% at 569 $\pm$ 42 μatm, 49 $\pm$ 60% at 1654 $\pm$ 112 μatm). At 5.2°C mean relative calcification was increased by $\sim$ 50% compared to the baseline at 583 $\pm$ 59 μatm, was decreased at intermediate pCO_2 levels and was increased again to the 100% baseline value at the highest pCO_2 level (1479 $\pm$ 93 μatm). Mean relative calcification at 7.5°C was increased compared to the baseline at 881 $\pm$ 65 μatm and was decreased at the two high pCO_2 levels with a minimum of -14 $\pm$ 88% compared to the baseline at 1422 $\pm$ 70 μatm (fig. 22).

In summary, highest relative calcification rates occured in the first two treatment phases and at the lowest and first elevated pCO_2 level (569μatm and 920 μatm) at 5.2°C and 7.5°C. Lowest relative calcification rates occured in the last treatment phase and at the highest pCO_2 level (1422 $\pm$ 70 μatm) at 7.5°C. Relative calcification rates at 3.4°C were constantly reduced over all treatment phases and at all pCO_2 level.

Data were normally distributed (Shapiro-Wilks test). We found no statistical significant effect of elevated temperature or CO_2 on net calcification; the effect of elevated CO_2 on net calcification was close to significance (p-value = 0.07) (compare tab. 3).

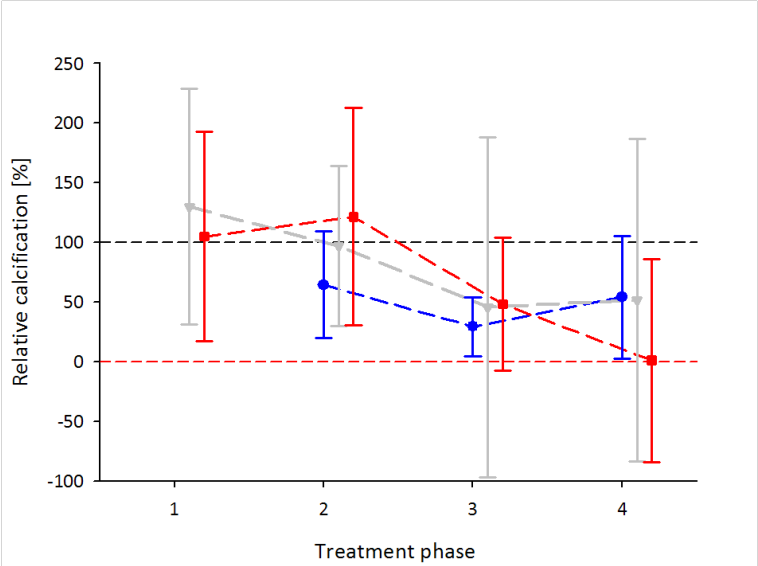

Figure 21: Mean relative calcification of *L. glaciale* over treatment duration (in treatment phases) (total alkalinity technique (Smith & Key, 1975)). Data points are means of pooled CO_2 and temperature treatments (12 combinations with each 4 measurements) from each one treatment phase. Standard deviations (± SD) are plotted against treatment duration (phases). Relative rates are normalized to rates of each individual alga under ambient conditions (3.4 ± 0.1°C, 568 ± 41 μatm: baseline). The black dashed reference line at 100% indicates the baseline rate. The red dashed reference line at 0.0 mg $CaCO_3$ d^{-1} indicates zero calcification; negative calcification (dissolution) occures below 0.0 mg $CaCO_3$ d^{-1}.

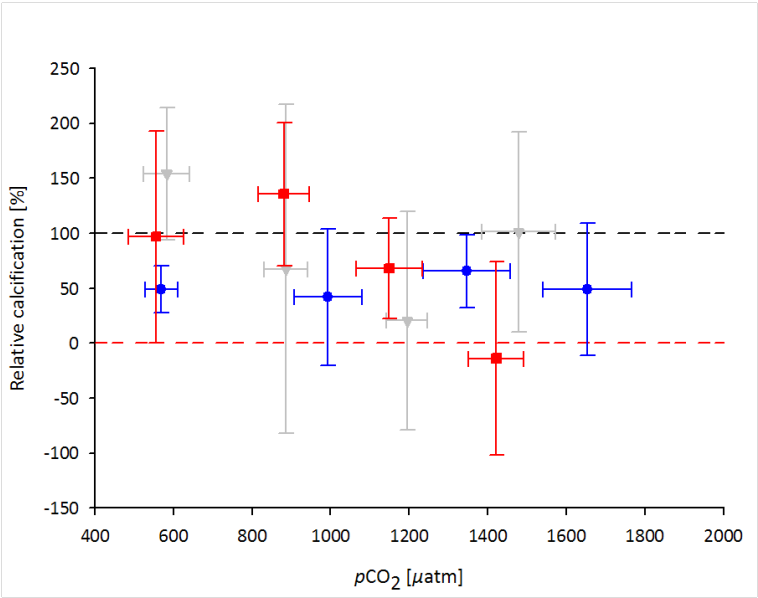

Figure 22: Mean relative calcification of *L. glaciale* with pCO_2 (total alkalinity method (Smith & Key, 1975)). Data points are means (n = 24) of pooled CO_2 of each temperature treatment over the experimental duration (blue = 3.4°C, grey = 5.2°C, red = 7.5°C). Standard deviations (± SD) are plotted against pCO_2. Relative rates are normalized to rates of each individual alga under ambient conditions (3.4 ± 0.1°C, 568 ± 41 μatm: baseline). The black dashed reference line at 100% indicates the baseline rate. The red dashed reference line at 0.0 mg $CaCO_3$ d^{-1} indicates zero calcification; negative calcification (dissolution) occures below 0.0 mg $CaCO_3$ d^{-1}.

3.7 Photosynthetic O_2 Evolution and Respiratory O_2 Consumption

Net photosynthetic O_2 evolution (O_2E) and respiratory O_2 consumption (O_2C) rates were measured in light, respectively dark. Relative rates (%) were calculated according to eq. 8. Actual mean temperatures of the temperature treatment during the O_2 measurements were 3.9 ± 0.5°C, 4.8 ± 0.7°C and 8.5 ± 0.1°C. Actual temperatures did not meet target temperatures of 3.5°C, 5.5°C and 7.5°C. With regard to their standard deviations, 3.9°C and 4.8°C were still in the temperature range of actual treatment temperatures (compare 3.3), whereas 8.5°C was 1°C warmer than the actual treatment temperature.

Mean relative O_2C rates were constant over experimental duration and with increasing pCO_2. Mean relative O_2C rates were significantly decreased ($p = 0.00$) with increasing temperature level. Relative O_2C rates at 3.9°C and 4.8°C were increased compared to the baseline, whereas relative O_2C rates at 8.5°C were decreased compared to the baseline. At 3.9°C relative O_2C rates were highest with a rate increase of 113 ± 9%. At 8.5°C relative O_2C rates were lowest with 92 ± 12%. The rate increase of the intermediate temperature 4.8°C was with 108 ± 8% lower than at 3.4°C and higher than at 8.5°C (fig. 23).

Mean relative O_2E rates were constant over the experimental duration, but decreased slightly with increasing pCO_2 (fig. 24). Relative O_2E rates were highest at the lowest and the first elevated pCO_2 level and were slightly decreased in the two highest pCO_2 levels. Looking at the temperature treatment, mean relative O_2E rates at 3.9°C were reduced ($\prec$100%) at all pCO_2 levels. Mean relative O_2E rates at 4.8°C were highest (190%) at the lowest pCO_2 and decreased with increasing pCO_2 to rates ($\prec$ 100%) in the highest pCO_2. At 8.5°C, mean relative O_2E rates were lowest (60%) in the lowest pCO_2 level and increased in the first elevated pCO_2 level to the highest measured rate increase (205%); with increasing pCO_2, mean relative O_2E rates decreased and increased again without a constant trend in regard to pCO_2.

Data of O_2E and O_2C were normally distributed (Shapiro-Wilks test) (after root-transformation for O_2E rates). We found a statistically significant effect of temperature on relative O_2C rates. We found no statistically significant effect of CO_2 on O_2C rates, or of CO_2 and temperature on relative O_2E rates (compare table 3).

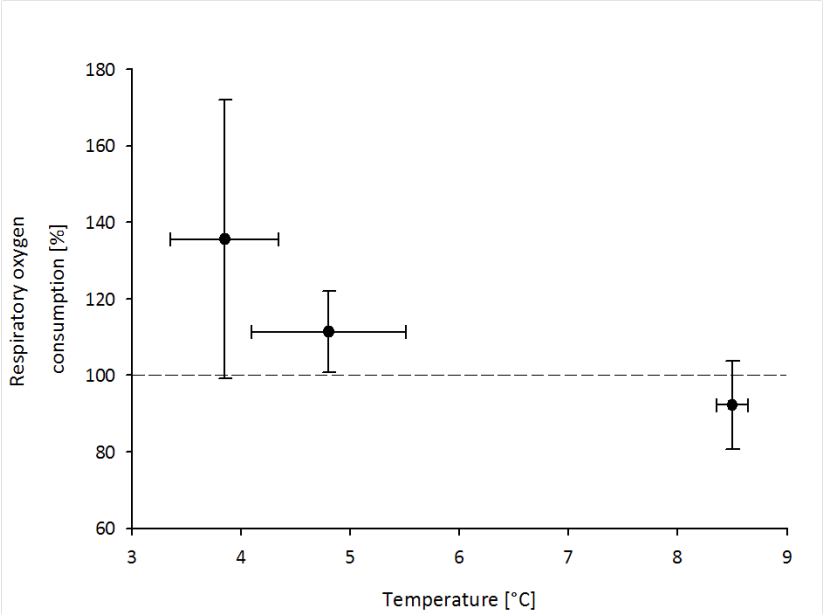

Figure 23: Mean relative respiratory O_2 consumption of *L. glaciale* with temperature. Data points are means of pooled CO_2 treatment (4 CO_2 levels with 1 measurements) from two treatment phases. Standard deviations (± SD) are plotted against the temperature treatment. Horizontal error bars give the SD of the temperature over the experimental duration. Relative rates are normalized to rates of a group of four algae under ambient conditions (baseline). The black dashed reference line at 100% indicates the baseline rate.

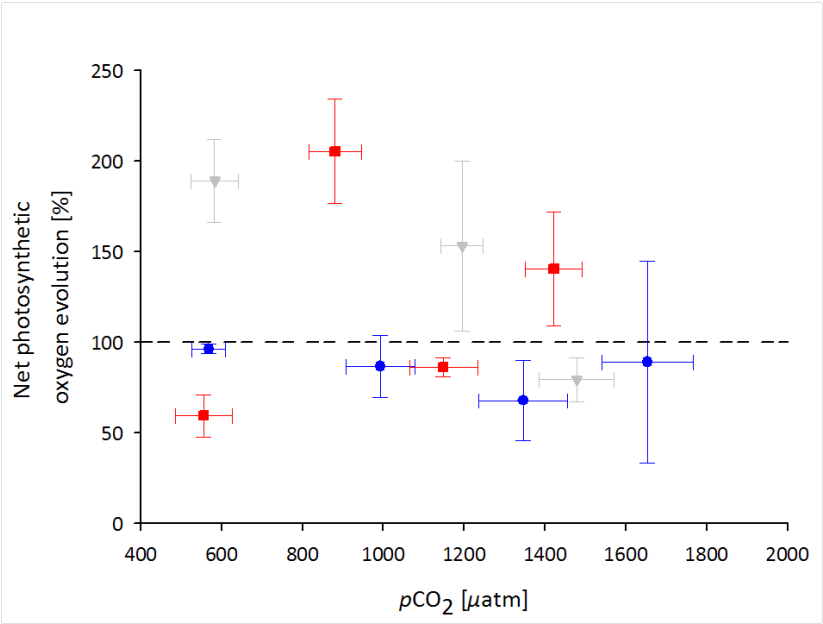

Figure 24: Mean relative net photosynthetic O_2 evolution of *L. glaciale* with pCO_2. Data points are means (n = 2) of pooled CO_2 of each temperature treatment over the experimental duration (blue = 3.9°C, grey = 4.8°C, red = 8.5°C). Standard deviations (± SD) are plotted against pCO_2. Relative rates are normalized to rates of a group of four algae under ambient conditions (baseline). The black dashed reference line at 100% indicates the baseline rate.

Table 3: Results of applied statistics: p-values of normal distribution (normality) and treatment effects (CO_2 and temperature) of measurement data. P-values $\succ 0.05$ support null hypothesis (H_0), p-values $\prec 0.05$ do not support H_0 and indicate significance.

	Normality		Treatment effect		
	Statistic	p-value	Statistic	p-value	
				CO_2	Temp.
Nutrient uptake	Shapiro-Wilks	0.83	Fact. Regress. Analysis	0.22	0.00
Buoyant weight	Shapiro-Wilks	0.86	MANOVA	0.10	0.13
Total alkalinity	Shapiro-Wilks	0.77	MANOVA	0.07	0.22
Photosynthetic O_2 evolution	Shapiro-Wilks	0.25	Fact. Regress. Analysis	0.98	0.50
Respiratory O_2 consumption	Shapiro-Wilks	0.62	Fact. Regress. Analysis	0.60	0.00

3.8 Applied Statistics

Table 3 gives a summary on applied statistical tests and according results.

4 Discussion

4.1 Identification

Algal specimens were identified to be of the genus *Lithothamnion* based on two vegetative features: 1. flared epithallial cells and 2. cell-fusions in the absence of secondary-pit connections. Most diagnostic features of the used identification key from Harvey & Woelkerling (2007) relate to reproductive features, which could not be identified in our algal specimens. However, among rhodolith forming genera the combination of the two identified vegetative features is only present in the genus *Lithothamnion* (Harvey & Woelkerling, 2007). The only other rhodolith forming genus having flared epithallial cells is *Sporolithon*, but in combination with secondary-pit connections (Harvey & Woelkerling, 2007). A mistaken identity between both genera was considered unlikely due to differences in secondary-pit connections and the fact that *Sporolithon* is not described to occur in Spitzbergen (Guiry & Guiry, 2012). Algal specimens were identified by means of the mean surface cell diameter to belong to the species *L. glaciale*.

4.2 Photo Database

Photos of the algal specimens taken at the end of the experiment revealed white spots and a brown film on algal surfaces. "Bleaching" (Webster *et al.*, 2011) of coralline algae is often noticed when algae are environmentally (Foster, 2001) or thermally stressed, e.g. at elevated temperatures (Webster *et al.*, 2011). Bleaching can be associated with the loss of photosynthetic pigments (Wilson *et al.*, 2004) and with dead tissue (Martin & Gattuso, 2009).

By the end of the experiment all incubated algae had white spots on their surfaces, indicating that they were stressed over the experimental duration. White spots did not seem to be particular abundant at elevated temperature compared to control temperature. It was shown that temperature stress increases the abundance of white spots (Webster *et al.*, 2011). Therefore, we would have expected the highest abundance of white spots on alga in the 7.5°C treatment, when associating 7.5°C with thermal stress for the algae. However, it has to be kept in mind, that the abundance of white spots was not quantitatively assessed.

The brown film was considered to result from biofouling, being a common process in the marine habitat (Wahl, 1989) and well known on coralline algae (Lewis *et al.*, 1985, Johnson *et al.*, 1991). Fouling epibionts were assumed to include bacteria (Lewis *et al.*, 1985, Johnson *et al.*, 1991), uni- and multicellular algae (Wahl, 1989). We did not clean algal specimens prior to or during the experiment as we considered it unpossible to remove all epibionts without harming the algae's surfaces. Therefore, it is assumed, that algal surfaces had already a biofilm of epibionts before the experiment started

which likely further grew over the experimental duration. In nature, coralline algae rely on grazers and sloughing to keep their surface clean (compare 1.3.2). During the experiment no grazers were present.

4.3 Nutrient Uptake

Concentrations of Si and $PO_4{}^{3-}$ did not change over the experimental duration. Si was not taken up during the experiment, indicating that silicifying algae were absent or of minimal abundance in the incubated water and on algal surfaces. Constant Si concentrations were expected as coralline algae do not take up Si. $PO_4{}^{3-}$ concentrations were at the detection limit and therefore no trend could be identified. Arctic waters are known to have low nutrient concentrations (Kirst & Wiencke, 1995), which was also the case during algal collection in Kongsfjorden (EPOCA 2010, unpublished data). Because the calcification process might support nutrient acquisition due to the release of H^+, McConnaughey & Whelan (1997) proposed that calcifying plants could live at very low nutrient concentrations.
The uptake of ΣN increased over experimental duration. Most likely, incubated algae where not the source for this increased uptake of ΣN, since for example calcification rates, which definitely related to coralline algae, did not increase accordingly (4.6). It is more likely, that the increasing uptake of ΣN was governed by a growing biofilm on the surface of incubated algae as indicated by a brownish film, which was visible on post-experimental pictures (4.2).
The mean relative uptake of ΣN did not change with increasing pCO_2 levels, indicating that uptake of ΣN was not affected by a decreasing pH.
The mean relative uptake of ΣN changed with temperature, being higher at 3.4°C than at 7.5°C. This finding was unexpected, as elevated temperatures usually enhance physiological processes (Sommer, 1998). A reason for reduced uptake of ΣN at 7.5°C might be temperature stress of incubated alga *Lithothamnion glaciale*, possibly affecting also its surface associated biofilm.
Uptake of ΣN had a large standard deviation. Assuming that the uptake of ΣN might be mostly governed by an epibiontic biofilm, this variation in uptake might be a consequence of different area covers of the biofilm.

In summary, for two reasons it is most likely that increasing uptake of ΣN resulted from a growing epibiontic biofilm on the surface of incubated coralline algae: 1. growth of a biofilm could be identified by comparing post- with pre-experimental pictures of algae; 2. uptake rates of ΣN did not correlate with coralline algae specific processes, e.g. calcification rates. Low uptake of ΣN at the highest temperature level was in accordance with reduced respiration rates, indicating energy limitation, e.g. for nutrient uptake mechanisms.

4.4 Carbonate System

Actual pCO_2 levels calculated from pH and total alkalinity (TA) measurements were higher than target levels. The lowest CO_2 level was intended to represent in-situ conditions of 390 μatm. Instead, we observed a pCO_2 of $\sim$ 560 μatm, which was nearly 50% higher than intended. This means, that we had no in-situ CO_2 level. Elevated CO_2 levels had an offset of $\sim$ 380 μatm each. Standard deviations of mean CO_2 levels did not overlap. Therefore, we still obtained four distinct CO_2 levels.

For the CO_2 treatment, we used CO_2 enriched air from gas mixing pumps, whose actual CO_2 concentrations were tested with a gas detector (GDZ401, Gas-Detektions-Zentrale) and were found to be in the range of target levels. pH was measured at the end of each incubation period, therefore, CO_2 equilibration of incubation water can be considered completed. pH changes due to biological activity were regarded unlikely as water was constantly aerated during incubation. The pH probe was regularly calibrated; measured pH data was corrected with measurements of certified reference material for ocean carbonate measurements (Prof. A.G. Dickson, Marine Physical Laboratory, University of California) (2.5.2). TA measurements of start values had a precision of 2.7 μmol kg^{-1}.

Consequently, we consider it most likely, that too high actual pCO_2 levels were caused by errors in the pH correction measurements of reference material. For example, a too short equilibration time of the pH probe could have resulted in a not representative pH which was subsequently used for the correction of measured sample pH from the experiment. Using a wrong correction factor might explain why all pCO_2 levels had nearly the same offset.

The incubation water was undersaturated with respect to Ω_{Ar} at all temperatures in the CO_2 enriched treatment levels. Water of the lowest CO_2 level was still saturated with respect to Ω_{Ar} at all temperatures (1.0 - 1.5, see tab. 2). Since *L. glaciale* contains 13 - 25% $MgCO_3$ (Kamenos *et al.*, 2008), being at least 20% more soluble than aragonite (Morse *et al.*, 2006), it is most likely that incubated algae at all CO_2 levels experienced undersaturation with respect to high Mg-calcite.

4.5 Calcification

We measured net calcification with both the buoyant weight (Davies, 1989) and the total alkalinity technique (Smith & Key, 1975). Calcification measured via buoyant weight is a direct measurement of changes in the $CaCO_3$ amount of calcified organisms, whereas calcification measured via total alkalinity is an indirect measurement of changes in carbonate chemistry of incubation water.

We found an overall good agreement of both techniques. The general CO_2 trend of calcification was the same between both techniques: calcification rates were highest at the two lowest pCO_2 levels and decreased with increasing pCO_2 in the elevated temperature levels.

A difference between both calcification rates was, that dissolution at 7.5°C in the highest pCO_2 level in the last treatment phase, was only visible in the higher temporal resolution of the total alkalinity technique. Since calcification rates calculated from the buoyant weight technique presented start and end changes, only positive rates were measured: Higher net calcification during treatment phase 1 to 3 compared to net dissolution in treatment phase 4 resulted in positive net calcification with respect to the total experimental duration. Furthermore, calcification rates obtained via the buoyant weight technique were two to four times higher than rates obtained with the total alkalinity technique. This finding could not be explained, so far. Which method to use depends on the study question and design. The high variation in calcification data obtained with the buoyant weight technique is assumed to be caused by different growth rates based on different surface areas of algal specimens. Growth in coralline algae is limited to the meristematic cell-layers close to the surface (Potin *et al.*, 1990) (1.3.1), i.e. the amount of meristematic cells and consequently the potential of growth increases with surface area. Large standard deviations of coralline algal growth obtained with the buoyant weight technique were also found in a study of Jokiel *et al.* (2008). To compare our algal growth ($CaCO_3$ deposition) with annual algal growth measured by Jokiel *et al.* (2008), we calculated only summer growths of tropical algae from Jokiel *et al.* (2008), since growth rates from our study are not representative for Arctic winter conditions. Tropical coralline algae had calcification rates of 200 ± 100 mg 4 $month^{-1}$ at ambient pCO_2 compared to calcification rates of 76 ± 42 mg 4 $months^{-1}$ at the lowest pCO_2 for polar coralline algae in our experiment. Growth in our algae was lower than growth obtained by Jokiel *et al.* (2008), what was expected due to lower (polar) experimental temperatures.

Treatment effects on *L. glaciale* were evaluated by looking at relative calcification rates. Relative calcification rates can be quantitatively evaluated since they are normalised to baseline rates for each individual algae (2.2).

Mean relative calcification of coralline algae measured via the total alkalinity technique decreased with experimental duration. This might be due to undersaturation of high Mg-calcite in all treatments. Undersaturated conditions were shown to affect calcification in coralline algae due to enhanced dissolution (Anthony *et al.*, 2008, Büdenbender *et al.*, 2011). Consequently, experimental duration equaled the duration of undersaturation with respect to high Mg-calcite, possibly promoting a decrease in calcification rates. Additionally, a mean decreasing relative calcification could be further promoted by the growing biofilm, e.g. due to shading.

Mean relative calcification decreased with experimental duration differently between temperatures with the strongest decrease at highest temperature, indicating an negative effect of elevated temperatures on calcification rates. A similar response was shown by Anthony *et al.* (2008) for tropical coralline algae: calcification rates at 3°C elevated temperatures were stronger reduced than at ambient

temperatures.

Mean relative calcification rates at 7.5°C increased until the second treatment phase and from then on decreased over the remaining treatment phases. The same pattern was also visible in the mean relative calcification response with respect to CO_2 levels. Relative mean calcification at 7.5°C increased from the lowest (556 ± 70 μatm) to the first elevated pCO_2 (881 ± 65 μatm) and decreased in the second and highest pCO_2 (1422 ± 70 μatm). This pattern of increasing calcification rates at intermediate pCO_2 and net dissolution at highest pCO_2 was already described by Ries *et al.* (2009) as "parabolic response", occuring i.a. in coralline algae (range of intermediate and highest pCO_2 given by Ries *et al.*: 409 ± 6 - 903 ± 12 μatm, respectively 2856 ± 54 μatm). Ω_{Ar} for intermediate and highest treatments applied by Ries *et al.* (2009) fit to Ω_{Ar} levels calculated for our 5.5°C and 7.5°C treatment (see tab. 2). Therefore, calcification responses are comparable. A parabolic response was also found by Büdenbender *et al.* (2011) in their study on *L. glaciale*. Ries *et al.* (2009) explains parabolic responses with an ability of organisms to regulate pH at the site of calcification (McConnaughey & Whelan, 1997), organic coating of calcified layers and photosynthetic activity. Yet, all algae were of the same species and would consequently all have pH-regulation of calcification and an organic coating (cell membrane) enclosing deposited $CaCO_3$, independent from the temperature of incubation, while only calcification at 7.5°C had a parabolic response. In regard to photosynthetic activity as explanation for a parabolic response, relative net photosynthetic rates at 5.5°C and 7.5°C peaked at the same pCO_2 as relative calcification rates did (parabolic response). It could be argued, that at increased net photosynthetic rates more energy (ATP) was produced at respective pCO_2, which could be subsequently used for the energy dependent pH regulation mechanism (McConnaughey & Whelan, 1997), enabling algae at 7.5°C to increase their calcification. Yet, inspite of elevated relative net photosynthetic rates at 5.2°C, algae from this treatment did not show a parabolic response. Reasons are unclear.

Mean relative calcification at 3.4°C was not affected by increasing CO_2 levels, but rates were reduced compared to the baseline, indicating a constant factor limiting calcification efficiency. That could mean that alga at 3.4°C were possibly negatively affected by elevated pCO_2, but were in all four CO_2 treatments able to cope with the CO_2 stress as relative calcification rates were constant at increasing CO_2 levels. Decreased calcification compared to the baseline might also have been affected by overgrowth of the discussed epiphytic biofilm (see 4.2).

Mean relative calcification at 5.2°C decreased with increasing pCO_2. An increased mean relative calcification at the lowest pCO_2 compared to baseline rates might indicate a positive temperature effect at low CO_2 levels (compare 7.5°C treatment). At the highest CO_2 level mean relative calcification was unexpectedly the same as in the baseline, which can not be explained by now.

In summary, calcification rates decreased over experimental duration and responded temperature-dependent differently to increasing pCO_2 levels, indicating a synergistic effect of both treatment factors. Algae at 3.4°C seem to be unaffected of increasing pCO_2 levels but at a reduced but still positive calcification rate. Algae at 7.5°C showed a parabolic response to increasing pCO_2 levels, resulting in net dissolution in the highest CO_2 level. Dissolution was only found in algae at 7.5°C and the highest pCO_2 (1422 $\pm$ 70 μatm) at the end of the experimental duration, indicating a synergistic effect of high CO_2 and high temperature levels.

4.6 Photosynthetic O_2 Evolution and Respiratory O_2 Consumption

Photosynthetic O_2 evolution (O_2E) and respiratory O_2 consumption (O_2C) of coralline algae under experimental treatment conditions were measured via changes in O_2 concentration in light and dark in the surrounding medium. According to Hofmann *et al.* (2011) O_2 evolution measurements in a closed water volume represent physiological responses as they directly measure a product of photosynthesis (O_2).

The highest temperature level during the O_2 measurements was 1°C higher than the according temperature level of the experimental treatment, likely due to the different measurement set-up. To compare O_2 measurements with calcification and nutrient uptake rates, we will treat actual temperatures of the O_2 measurements the same as actual treatment temperatures. Although a temperature difference of 1°C is assumed to likely change net measured rates particular for O_2C rates (statistical significant temperature effect), it might be argued, that O_2C rates would have been similar low at a 1°C lower temperature than at the actual temperature (8.5°C). This might be assumed due to the decreasing trend of O_2C rates (compare 23).

Relative net photosynthetic O_2 evolution (O_2E) rates were not affected by CO_2. It might have been expected, that relative O_2E rates would increase with increasing pCO_2 due to a higher substrate availability for the photosynthesis with respect to dissolved inorganic carbon (DIC) (photosynthetically used: CO_2 and HCO_3^-) (Riebesell *et al.*, 2007).

We found a similarity between relative O_2E and relative calcification rates: with few exceptions, relative O_2E rates had a similar pattern with increasing CO_2 as relative calcification rates in the respective temperature treatments. Both rates were 20 - 50% reduced at 3.4°C, decreased with increasing pCO_2 at 5.2°C and had a parabolic response at 7.5°C with highest rates at the second CO_2 level. Only relative O_2E at 7.5°C and 1500 μatm and relative calcification at 5.5°C and 1500μatm did not fit to described trends. Similarities between relative O_2E and relative calcification rates might indicate a coupling of both processes, i.e. photosynthetis and calcification in the coralline alga *L. glaciale* seem to be closely connected. However, the driving factors remain unclear. In order to distinguish whether

calcification, or temperature and CO_2 affect photosynthesis, a future experimental design should also include uncalcified algae.

Relative respiratory O_2 consumption (O_2C) decreased significantly with increasing temperatures. Since physiological processes generally increase with increasing temperature (Sommer, 1998), respiration rates were expected to increase with increasing temperature. In our experiment, we observed the opposite effect: at the highest temperature (7.5°C) the lowest respiration rates were measured. This reverse finding might indicate a temperature dependence of algal respiration rates: *L. glaciale* in our experiment could have been stressed by increasing temperature to an extend where basic physiological activity, like respiration, was negatively affected. Temperature stress in algae at 7.5°C was also already discussed for decreased ΣN uptake rates (4.4) and decreased calcification rates (4.6.2).

Respiration allocates energy for energy consuming processes (Sommer, 1998), like growth or calcification in coralline algae (Okazaki, 1977). Low respiration rates of algae at 7.5°C could consequently mean that less energy was available for their metabolic processes. Limited energy availability at 7.5°C could be an explanation for decreasing calcification rates with increasing CO_2. In the same way, sufficient energy availability due to increased respiration at 3.4°C might explain the reduced but constant calcification rates with increasing CO_2: Calcification in coralline algae is supposed to be an energy dependend process (Okazaki, 1977). A likely mechanism promoting the calcification process is the active redulation of pH at the site of calcification, being proposed to occur in coralline algae (McConnaughey & Whelan, 1997). An increasing pH might possibly promote the conversion from HCO_3^- to CO_3^{2-}, which is an important substrate in the calcification process (Borowitzka, 1982a). pH regulation is assumed to be energy dependent, for example due to active transport mechanisms of H^+ (McConnaughey & Whelan, 1997). Consequently, when energy availability is limited, e.g. due to reduced respiration rates, likely only limited energy can be used for the regulation of pH, which could affect CO_3^{2-} availability and therefore the calcification process. At increased CO_2 levels pH regulation might be of even higher importance for the calcification process by providing suitable conditions for the conversion of HCO_3^- to CO_3^{2-}. Since CO_3^{2-} concentrations are already low, reduced calcification due to energy limitation could further decrease net calcification and possibly result in net dissolution, as dissolution rates are likely increased at increased pCO_2 levels. This could have been the case for algae at 7.5°C, which had reduced respiration rates and experienced net dissolution at the highest pCO_2 (Ω_{Ar} 0.63 ± 0.03). However, it remains unclear, why thermal stress might led to reduced respiration rates.

In summary, results of photosynthetic O_2 evolution indicate a linkage between photosynthesis and calcification. Based on our results, increased temperature seems to impair algae respiration rates.

5 Conclusion

In this study, we investigated single as well as synergistic effects of ocean warming (OW) and ocean acidification (OA) on calcification and photosynthesis of the Arctic coralline red alga *Lithothamnion glaciale* under Arctic summer light conditions. We were interested in whether 1. OW would interact with reported negative OA effects on calcification 2. calcification would correlate with photosynthesis or respiration, indicating a likely linkage between these processes and 3. which implications could be drawn out of our findings for *L. glaciale* under future ocean conditions.

The effects of increasing temperature and increasing pCO_2 on *L. glaciale* were tested by incubating algal specimens from the Kongsfjord, Spitzbergen for two months under a treatment of elevated pCO_2 (569 - 1518 μatm) and elevated temperature (3.4 - 7.5°C). Treatment levels were designed to represent future conditions of OW and OA modeled for the Arctic Ocean (Steinacher *et al.*, 2009) based on emission scenario SRES A2 (IPCC, 2000). The extreme conditions of the highest treatment level, being elevated by + 4°C and + 1200 μatm compared to ambient conditions, were exceptions to model predictions and applied in order to increase the likelihood for the observation of physiological responses. The lowest treatment level was designed to represent in-situ conditions of the Arctic habitat of *L. glaciale* in summer. With respect to CO_2 concentrations, we failed to met these conditions because all observed CO_2 levels were higher than intended. However, treatment levels were still distinct with respect to CO_2. Irradiance simulated in-situ conditions of the Arctic summer season as experienced by investigated algae specimens (12 μmol photons m^{-2} s^{-1} for 24 h). The response of *L. glaciale* to the applied treatment was tested in regard to nutrient uptake, calcification and photosynthetic O_2 evolution (O_2E) and respiratory O_2 consumption (O_2C).

In the highest temperature treatment (7.5°C) relative nutrient uptake (ΣN), relative calcification and relative O_2C rates were decreased compared to the baseline. In contrary, in the lowest temperature treatment (3.4°C) relative uptake of ΣN and relative (O_2C) rates were increased. Relative calcification at 3.4°C was reduced compared to the baseline. The temperature treatment effects on algae were particular pronounced in relative calcification and O_2C rates: Calcification rates of algae at 7.5°C turned after an incubation time of 8 weeks only in the highest pCO_2 treatment into net dissolution, whereas calcification rates at 3.4°C were at a reduced rate but did not change over experimental duration and also not with increasing CO_2 level (min. Ω_{Ar} 0.45 $\pm$ 0.03). Mean relative O_2C rates at 7.5°C were reduced by 20% compared to rates at 3.4°C, indicating lower energy availability for algae at 7.5°C.

Reduced calcification and respiration rates at 7.5°C could indicate thermal stress, possibly inhibiting

metabolic efficiency (as discussed). Since *L. glaciale* is a dominant coralline alga species of the Subarctic Ocean (Adey *et al.*, 2005), it can be assumed that *L. glaciale* is likely adapted to low Arctic water temperatures. Therefore, an increase of mean surface sea temperature of circa 4°C was expected to establish temperature stress for *L. glaciale*.

The comparison of relative calcification and O_2C rates with respect to temperature levels indicated a possible temperature threshold between 5.2°C and 7.5°C, since *L. glaciale* seemed to be unable to sustain net calcification at high pCO_2 concentrations and simultaneously reduced respiration at 7.5°C. However, according to Adey (1970) the optimum growth temperature reported for *L. glaciale* ranges from 9 - 15°C, being higher than our highest temperature level. Büdenbender *et al.* (2011) proposed, that increased temperatures could promote calcification in the Arctic coralline alga *L. glaciale*. This hypothesis was supported by our study, since algae at + 2°C and + 4°C elevated temperature treatments experienced increased calcification rates at low and intermediate elevated CO_2 levels. However, at high CO_2 levels $\succ$ 1000 μatm this assumption did not hold true, since calcification at 7.5°C was circa 60% lower than at 3.4°C, resulting in net dissolution of respective algae.

With high CO_2 decreasing relative calcification rates and reduced O_2C rates at 7.5°C might indicate, that calcification rates could be affected by thermal stress via energy limitation. Energy is allocated during respiration (Sommer, 1998). Reduced O_2C rates could indicate reduced energy availability. Since calcification is assumed to be an energy dependent process, e.g. due to pH-regulation mechanisms as proposed by McConnaughey & Whelan (1997), calcification is likely affected by reduced energy availability. Energy limitation due to reduced O_2C caused by ocean warming could likely enhance effects of additional stressors, e.g. high CO_2 concentrations. Since energy limitation due to temperature stress had only an effect on calcification rates at very high pCO_2 ($\succ$ 1000 μatm), a synergistic effect between elevated temperatures and very high CO_2 is likely.

Within the temperature range of 3.4°C - 5.2°C relative O_2C rates were not reduced, what could mean that energy allocation was not reduced as well. Calcification in this temperature range was reduced but constant over experimental duration and reduced calcification rates could have been the result of undersaturated conditions with respect to high Mg-calcite. However, the constance in reduced calcification with CO_2 seems to indicate, that alga could withstand increasing pCO_2 stress, possibly due to sufficient energy availability.

Relative calcification and photosynthetic O_2 evolution (O_2E) rates showed a similar pattern, indicating a close linkage between both processes. Since photosynthesis is ultimately the energy providing process in transferring light energy into organic energy, the linkage could be the same as discussed for relative O_2C rates.

In summary, calcification in *L. glaciale* seems to be linked to energy availability and therefore to energy generating processes, like photosynthesis and respiration. Under reduced energy availability, calcified algae as *L. glaciale* seem to be more susceptible to net dissolution at high pCO_2, as shown in this study at 7.5°C and 1518 μatm. This finding indicates a synergistic effect of temperature and pCO_2 on calcification.

Since highest simulated OW and OA of + 4°C and + 1200 μatm are not expected to occur in the Arctic surface ocean in the near future (Steinacher *et al.*, 2009), *L. glaciale* might not experience reduced calcification during the summer season within this century. In contrast, calcification of *L. glaciale* could be promoted by a temperature elevation of + 2°C at moderately increased CO_2 concentrations (up to 560 μatm).

However, it has to be kept in mind, that given results relate to Arctic summer light conditions of 24 h irradiance, being the highest amount of light available in the course of a year. Responses to the applied treatment are likely different under Arctic winter conditions of 24 h darkness. Without light, photosynthesis and consequently energy fixation cannot take place. Respiration rates are assumed to be reduced in order to limit energy consumption as stored photosynthates have to last for the whole winter period. Due to continuous energy limitation, calcification rates of *L. glaciale* are expected to be strong affected with respect to CO_2 during the Arctic winter. To evaluate implications for the Arctic benthic ecosystem, the same study should be repeated under Arctic winter conditions.

From this study one can conclude, that within this century the Arctic coralline alga *Lithothamnion glaciale* might not be negatively affected by elevated temperatures and pCO_2 during the Arctic summer season, but rather might profit from those conditions by increasing its calcification rates.

Negative effects of elevated temperatures and pCO_2 on *L. glaciale* during the Arctic summer season are first expected for a combination of temperature and pCO_2, that is not predicted to occur within this century for the Arctic Ocean.

6 Acknowledgement

This work was made possible by Prof. Ulf Riebesell, whom I want to thank for giving me the chance to conduct my thesis in his working group. Further, I want to thank Prof. Frank Melzner for reviewing this work as second supervisor.

Most of all I want to thank my supervisor Jan Büdenbender, who introduced me thoroughly and patiently to experimental working and was always helpful at potential scientific pitfalls. He supported me in both the practical and analytic part of the experiment, and gave me useful comments on my scientific writing, pushing me to improve myself. He always had an open ear, an open mind and great motivation.

Further I want to thank Dr. Armin Form, who helped in the oxygen measurements, having always time on his hand, good advice and a lot of equipment.

A big thank you to Paul Stange, who helped in measuring the mass amounts of alkalinity samples and endured all those days in a lab without windows. Thanks to Kerstin Nachtigall, who introduced me to nutrient measurements with the autoanalyzer and helped in measuring the samples. Thanks to the TLZ for allowing Jan and me to build our experimental reactors in their space, and special thanks to Dirk Wehrend for introducing us patiently and just marginal worried to the world of precision mechanics. Thanks to Sarah Febiri for proof reading and good advice.

Thanks to the working group of Biological Oceanography for answering all my questions and helping with advice and time for a chat. Special thanks to my office mates of room 218 for fun, friendship, support and the never ending open-window fights.

Finally, I want to thank my friends for positive distraction, motivation and their patience in listening to all those talks dominated by thesis issues. Thanks to my modelling friends for introducing me to LaTex. Special thanks to my family for enduring love, trust and support.

References

ACIA (2005) Arctic Climate Impact Assessment. Arris L (ed), Cambridge University Press, Cambridge, 1042 pages.

Adey WH (1970) The effects of light and temperature on growth rates in boreal-subarctic crustose corallines. J Phycol 6: 269-276.

Adey WH, Macintyre IG (1973) Crustose coralline algae: a re-evaluation in the geological sciences. Geol Soc Am Bull 84: 883-904.

Adey WH, Chamberlain YM, Irvine LM (2005) An sem-based analysis of the morphology, anatomy, and reproduction of *Lithothamnion tophiforme* (Esper) Unger (Corallinales, Rhodophyta), with a comparative study of associated north Atlantik Arctic/Subarctic Melobesioideae. J Phycol 41: 1010-1024.

Andersson AJ, Mackenzie FT, Bates NR (2008) Life on the margin: implications of ocean acidification on Mg-calcite, high latitude and cold-water marine calcifiers. Mar Ecol Prog Ser 373: 265-273.

Anthony KRN, Kline DI, Diaz-Pulido G, Dove S, Hoegh-Guldberg O (2008) Ocean acidification causes bleaching and productivity loss in coral reef builders. Proc Natl Acad Sci USA 105: 17442-17446.

Baker LM, Dunbar K (2000) Experimental design heuristics for scientific discovery: the use of "baseline" and "known standard" controls. Int J Human-Comp Stud 53: 335-349.

Barnett TP, Pierce DW, AchutaRao KM, Gleckler PJ, Santer BD, Gregory JM, Washington WM (2005) Penetration of human-induced warming into the World's ocean. Science 309: 284-287.

Bilan MI, Usov AI (2001) Polysaccharides of calcareous algae and their effect on the calcification process. Russ J Bioorg Chem 27: 2-16.

BIOMAERL Team (2003) Conservation and management of northeast Atlantic and Mediterranean maerl beds. Aquatic Conserv: Mar Freshw Ecosyst 13: S65-S76.

Bopp L, Monfray P, Aumont O, Dufresne J-L, Treut HL, Madec G, Terray L, Orr JC (2001) Potential impact of climate change on marine export production. Global Biogeochem Cycles 15: 81-99.

Borowitzka MA (1977) Algal calcification. Oceanogr Mar Biol Ann Rev 15: 189-223. Barnes H (ed), Aberdeen University Press.

Borowitzka MA (1982) Mechanisms in algal calcification. Prog Phycol Res 1: 137-177.

Borowitzka MA, Vesk M (1978) Ultrastructure of the Corallinaceae I. The vegetative cells of *Corallina officinalis* and *C. cuvierii*. Mar Biol 46: 295-304.

Bosence D, Wilson J (2003) Maerl growth, carbonate production rates and accumulation rates in the northeast Atlantic. Aquatic Conserv: Mar Freshw Ecosyst 13: S21-S31.

Büdenbender J, Riebesell U, Form A (2011) Calcification of the Arctic coralline red algae *Lithothamnion glaciale* in response to elevated CO_2. Mar Ecol Prog Ser 441: 79-87.

Caldeira K, Wickett ME (2003) Anthropogenic carbon and ocean pH. Nature 425: 365.

Canadell JG, Le Quéré C, Raupach MR, Field CB, Buitenhuis ET, Ciais P, Conway TJ, Gillett NP, Houghton RA, Marland G (2007) Contributions to accelerating atmospheric CO_2 growth from economic activity, carbon intensity, and efficiency of natural sinks. Proc Natl Acad Sci USA 104: 18866-18870.

Davies PS (1989) Short-term growth measurements of corals using an accurate buoyant weighing technique. Mar Biol 101: 389-395.

Dethier MN, Steneck RS (2001) Growth and persistence of diverse intertidal crusts: survival of the slow in a fast-paced world. Mar Ecol Prog Ser 223: 89-100.

Dickson AG (1981) An exact definition of total alkalinity and a procedure for the estimation of alkalinity and total inorganic carbon from titration data. Deep-Sea Res 28: 609-623.

Dickson AG (2011) Certificate of analysis: reference material for oceanic CO_2 measurements, batch 108 (bottled on November $10^{-}th$, 2010). Marine Physical Laboratory, Scripps Institution of Oceanography, University of California.

Dickson AG, Afghan JD, Anderson GC (2003) Reference materials for oceanic CO_2 analysis: a method for the certification of total alkalinity. Mar Chem 80: 185-197.

Dickson AG, Sabine CL, Christian JR (2007) SOP 6a Determination of the pH of sea water using a glass/reference electrode cell. In: Guide to best practices for ocean CO_2 measurements. Dickson AG, Sabine CL, Christian JR (eds), PICES Special Publication 3, 1-7.

Digby PSB (1977) Growth and calcification in the coralline algae *Clathromorphum circumscriptum* and *Corallina officinalis* and the significance of pH in relation to precipitation. J Mar Biol Assoc UK 57: 1095-1109.

ESRL/NOAA CO_2 data: http://www.esrl.noaa.gov/gmd/ccgg/trends/w.esrl/noaa, 14th March, 2012.

Riebesell U, Fabry VJ, Hansson L, Gattuso J-P (eds) (2010) Guide to best practices for ocean acidification research and data reporting. Publications Office of the European Union, Luxembourg, 260 pages.

Fabry VJ, Seibel BA, Feely RA, Orr JC (2008) Impacts of ocean acidification on marine fauna and ecosystem processes. Int Counc Explor Sea (ICES) J Mar Sci 65: 414-432.

Fofonoff P, Millard Jr RC (1983) Algorithms for computation of fundamental properties of seawater. UNESCO Technical Papers in Marine Sciences 44, 53 pages.

Form AU (2011) Influence of anthropogenic climate change on the ecophysiology of the cold-water coral *Lophelia pertusa*. Doctoral Thesis, Leibniz Institute of Marine Sciences (IFM-GEOMAR), Christian-Albrechts University, Kiel, 218 pages.

Foster MS (2001) Rhodoliths: between rocks and soft places. J Phycol 37: 659-667.

Freiwald A, Henrich R (1994) Reefal coralline algal build-ups within the Arctic Circle: morphology and sedimentary dynamics under extreme environmental seasonality. Sedimentology 41: 963-984.

Guinotte JM, Fabry VJ (2008) Ocean acidification and its potential effects on marine ecosystems. Ann NY Acad Sci 1134: 320-342.

Guiry MD, Guiry GM (2012) AlgaeBase. World-wide electronic publication, National University of Ireland, Galway. http://www.algaebase.org, 29th April, 2012.

Hanelt D, Tüg H, Bischof K, Gro C, Lippert H, Sawall T, Wiencke C (2001) Light regime in an Arctic fjord: a study related to stratospheric ozone depletion as a basis for determination of UV effects on algal growth. Mar Biol 138: 649-658.

Hansen JR, Jenneborg LH (1996) Part 7. Benthic marine algae and cyanobacteria. In: A catalogue of Svalbard plants, fungi, algae and cyanobacteria. Elvebakk A, Prestrud P (eds), Norsk Polarinstitutt Skrifter 198: 361-374.

Harvey AS, Woelkerling WJ (2007) Gua para la identificación de rodolitos de algas rojas coralinas no geniculadas (Corallinales, Rhodophyta). A guide to nongeniculate coralline red algal (Corallinales, Rhodophyta) rhodolith identification. Ciencias Marinas 33: 411-426.

Henderson C (2006) Ocean acidification: the other CO_2 problem. New Scientist: http://www.newscientist.com/article/mg19125631.200-ocean-acidification-the-other-co2-problem.html, 23rd March, 2012.

Hofmann LC, Yildiz G, Hanelt D, Bischof K (2011) Physiological responses of the calcifying rhodophyte, *Corallina officinalis* (L.), to future CO_2 levels. DOI 10.1007/s00227-011-1854-9.

Hop H, Pearson T, Hegseth EN, Kovacs KM, Wiencke C, Kwasniewski S, Eiane K, Mehlum F, Gulliksen B, Wlodarska-Kowalczuk M *et al.* (2002) The marine ecosystem of Kongsfjorden, Svalbard. Polar Res 21: 167-208.

IPCC (2000) Special report on emissions scenarios. A special report of working group III of the Intergovernmental Panel on Climate Change. Nakicenovic N, Swart R (eds), Cambridge University Press, Cambridge, 570 pages.

IPCC (2001) Impacts, adaptation and vulnerability. Contribution of working group II to the Third Assessment Report of the Intergovernmental Panel on Climate Change. McCarthy JJ, Canziani OF, Leary NA, Dokken DJ, White KS (eds), Cambridge University Press, Cambridge, 1032 pages.

Johansen HW (1981) Coralline algae, a first synthesis. CRC Press, Florida, 239 pages.

Johnson CR, Muir DG, Reysenbach AL (1991) Characteristic bacteria associated with surfaces of coralline algae: a hypothesis for bacterial induction of marine invertebrate larvae. Mar Ecol Prog Ser 74: 281-294.

Jokiel PL, Rodgers KS, Kuffner IB, Andersson AJ, Cox EF, Mackenzie FT (2008) Ocean acidification and calcifying reef organisms: a mesocosm investigation. Coral Reefs 27: 473-483.

Jokiel RL, Maragos JE, Franzisket L (1978) Coral growth: buoyant weight technique. UNESCO Monogr Oceanogr Methodol 5: 529-541.

Joos F, Spahni R (2008) Rates of change in natural and anthropogenic radiative forcing over the past 20.000 years. Proc Natl Acad Sci USA 105: 1425-1430.

Kamenos NA, Cusack M, Moore PG (2008) Coralline algae are global palaeothermometers with bi-weekly resolution. Geochim Cosmochim Acta 72: 771-779.

Key RM, Kozyr A, Sabine CL, Lee K, Wanninkhof R, Bullister JL, Feely RA, Millero FJ, Mordy C, Peng T-H (2004) A global ocean carbon climatology: results from Global Data Analysis Project (GLODAP). Global Biogeochem Cycles 18: GB4031.

Kirst GO, Wiencke C (1995) Ecophysiology of polar algae. J Phycol 31: 181-199.

Kleypas JA, Langdon C (2006) Coral reefs and changing seawater carbonate chemistry. Coast Estuar Stud 61: 73-110.

Kuffner IB, Andersson AJ, Jokiel PL, Rodgers KS (2008) Decreased abundance of crustose coralline algae due to ocean acidification. Nat Geosci 1: 114-117.

Levitus S, Antonov J, Boyer T (2005) Warming of the World ocean, 1955 - 2003. Geophys Res Lett 32: L02604.

Lewis E, Wallace DWR (1998) Program developed for CO_2 system calculations. ORNL/CDIAC-105: Carbon Dioxide Information Analysis Center, Oak Ridge National Laboratory, Oak Ridge, Tennessee.

Lewis TE, Garland CD, McMeekin TA (1985) The bacterial biota on crustose (nonarticulated) coralline algae from Tasmanian waters. Microb Ecol 11: 221-230.

Lind JW (1970) Processes of calcification in the coralline algae. Doctoral Thesis, University of Hawaii, Honolulu, 288 pages.

Littler MM (1972) The crustose corallinaceae. Oceanogr Mar Biol Ann Rev 10: 311-347.

Littler MM (1976) Calcification and its role among the macroalgae. Micronesica 12: 27-41.

Loeng H, Brander K, Carmack E, Denisenko S, Drinkwater K, Hansen B, Kovacs K, Livingston P, McLaughlin F, Sakshaug E (2005) Marine systems. In: ACIA (2005) Arctic Climate Impact Assessment. Arris L (ed) Cambridge University Press, Cambridge, 453-538.

Mackenzie FT, Bischoff WD, Bishop FC, Loijens M, Schoonmaker J, Wollast R (1983) Magnesian calcites: low-temperature occurrence, solubility and solid-solution behavior. Rev Mineral Geochem 11: 97-144.

Martin S, Gattuso J-P (2009) Response of Mediterranean coralline algae to ocean acidification and elevated temperature. Global Change Biol 15: 2089-2100.

McBean G, Alekseev G, Chen D, Førland E, Fyfe J, Groismann PY, King R, Melling H, Vose R, Whitfield PH (2005) Arctic climate - past and present. In: ACIA (2005) Arctic Climate Impact Assessment. Arris L (ed) Cambridge University Press, Cambridge, 21-60.

McConnaughey TA, Whelan JF (1997) Calcification generates protons for nutrient and bicarbonate uptake. Earth Sci Rev 42: 95-117.

Mitchell JFB (1989) The "greenhouse" effect and climate change. Rev Geophys 27: 115-139.

Morse JW, Andersson AJ, Mackenzie, FT (2006) Initial responses of carbonate-rich shelf sediments to rising atmospheric pCO_2 and "ocean acidification": role of high Mg-calcites. Geochim Cosmochim Acta 70: 5814-5830.

Nelson WA (2009) Calcified macroalgae - critical to coastal ecosystems and vulnerable to change: a review. Mar Freshw Res 60: 787-801.

Okazaki M (1977) Some enzymatic properties of Ca^{2+}-dependent adenosine triphosphatase from a calcareous red alga, *Serraticardia maxima*, and its distribution in marine algae. Botanica Mar 20: 347-354.

Orr JC, Fabry VJ, Aumont O, Bopp L, Doney SC, Feely RA, Gnanadesikan A, Gruber N, Ishida A, Joos F *et al.* (2005) Anthropogenic ocean acidification over the twenty-first century and its impact on calcifying organisms. Nature 437: 681-686.

Potin P, Floc'h JY, Augris C, Cabioch J (1990) Annual growth rate of the calcareous red alga *Lithothamnion corallioides* (Corallinales, Rhodophyta) in the Bay of Brest, France. Hydrobiologia 204/205: 263-267.

PreSens (2005) Instruction manual OXY-10: 10-channel fiber-optic oxygen meter, software version OXY 10v3_33FB. Precision Sensing GmbH.

Raupach MR, Marland G, Ciais P, Le Quéré C, Canadell JG, Klepper G, Field CB (2007) Global and regional drivers of accelerating CO_2 emissions. Proc Natl Acad Sci USA 104: 10288-10293.

Riebesell U, Zondervan I, Rost B, Tortell PD, Zeebe RE, Morel FMM (2000) Reduced calcification of marine plankton in response to increased atmospheric CO_2. Nature 407: 364-367.

Riebesell U, Schulz KG, Bellerby RGJ, Botros M, Fritsche P, Meyerhöfer M, Neill C, Nondal G, Oschlies A, Wohlers J, Zöllner E (2007) Enhanced biological carbon consumption in a high CO_2 ocean. Nature 450: 545-549.

Ries JB, Cohen AL, McCorkle DC (2009) Marine calcifiers exhibit mixed responses to CO_2-induced ocean acidification. Geology 37: 1131-1134.

Sabine CL, Feely RA, Gruber N, Key RM, Lee K, Bullister JL, Wanninkhof R, Wong CS, Wallace DWR, Tilbrook B, Millero FJ, Peng T-H, Kozyr A, Ono T, Rios AF (2004) The oceanic sink for anthropogenic CO_2. Science 305: 367-371.

Sarmiento JL, Slater R, Barber R, Bopp L, Doney SC, Hirst AC, Kleypas J, Matear R, Mikolajewicz U, Monfray P, Soldatov V, Spall SA, Stouffer R (2004) Response of ocean ecosystems to climate warming. Global Biogeochem Cycles 18: GB3003.

Schwarz A-M, Hawes I, Andrew N, Mercer S, Cummings V, Thrush S (2005) Primary production potential of non-geniculate coralline algae at Cape Evans, Ross Sea, Antarctic. Mar Ecol Prog Ser 294: 131-140.

Smith SV, Key GS (1975) Carbon dioxide and metabolism in marine environments. Limnol Oceanogr 20: 493-495.

Sommer U (1998) Biologische Meereskunde. Springer-Verlag, Berlin, Heidelberg, 475 pages.

Steinacher M, Joos F, Frölicher TL, Plattner G-K, Doney SC (2009) Imminent ocean acidification in the Arctic projected with the NCAR global coupled carbon cycle-climate model. Biogeosciences 6: 515-533.

Steneck RS (1986) The ecology of coralline algal crusts: convergent patterns and adaptive strategies. Annu Rev Ecol Syst 17: 273-303.

Svendsen H, Beszczynska-Møller A, Hagen JO, Lefauconnier B, Tverberg V, Gerland S, Ørbæk JB, Bischof K, Papucci C, Zajaczkowski M *et al.* (2002) The physical environment of Kongsfjorden - Krossfjorden, an Arctic fjord system in Svalbard. Polar Res 21: 133-166.

Tomczak P (2000) Seawater density calculator. www.es.flinders.edu.au/ mattom/Utilities/density.html, 25th March, 2012.

Usher MB, Callaghan TV, Gilchrist G, Heal B, Juday GP, Loeng H, Muir MAK, Prestrud P (2005) Principles of conserving the Arctic's Biodiversity. In: ACIA (2005) Arctic Climate Impact Assessment. Arris L (ed) Cambridge University Press, Cambridge, 539-596.

Vinogradov AP (1953) The elementary chemical composition of marine organisms. Sears Foundation for Marine Research, Yale University, New Haven, 647 pages.

Wahl M (1989) Marine epibiosis. I. Fouling and antifouling: some basic aspects. Mar Ecol Prog Ser 58: 175-189.

Webster NS, Soo R, Cobb R, Negri AP (2011) Elevated seawater temperature causes a microbial shift on crustose coralline algae with implications for the recruitment of coral larvae. The ISME Journal 2: 759-770.

Wilson S, Blake C, Berges JA, Maggs CA (2004) Environmental tolerances of free-living coralline algae (maerl): implications for European marine conservation. Biol Conserv 120: 279-289.

Woelkerling WJ (1988) The coralline red algae: an analysis of the genera and subfamilies of non-geniculate Corallinaceae. Oxford University Press, London, 268 pages.

Zeebe RE, Wolf-Gladrow D (2001) CO_2 in seawater: equilibrium, kinetics, isotopes. Elsevier Oceanography Book Series 65, Amsterdam, 360 pages.

Declaration on Oath

I hereby declare that I have completed the present master thesis "Effects of Warming and Ocean Acidification on Calcification and Photosynthesis of Arctic Coralline Red Algae under Summer Light Conditions" on my own without using others than the stated sources and auxiliary means.
The electronic version corresponds to this written version.
I assure that this thesis has not been submitted at other places to achieve the master's degree (M.Sc.).

I agree, that a copy of this thesis will be made available in the library of the Christian-Albrechts University, Kiel.

Kiel, 28^{th} April, 2012

Dana Hellemann